Rapid Morphologic and Molecular Activation of Microglial Cells by Stimulation of the P2X7 Receptor Correlates with Neuron Loss

Keith E Campagno
University of Pennsylvania
Wennan Lu
University of Pennsylvania
Assraa Hassan Jassim
University of Pennsylvania
Farraj Albalawi
King Saud bin Abdulaziz University for Health Sciences
Aurora Cenaj
University of Pennsylvania
Huen-Yee Tso
University of Pennsylvania
Sophia P Clark
University of Pennsylvania
Sripinun Puttipong
University of Pennsylvania
Néstor Más Gómez
University of Pennsylvania
Claire H Mitchell (chm@upenn.edu)
University of Pennsylvania https://orcid.org/0000-0002-9784-6672

Research Article

Keywords: Microglial activation, P2X7 receptor, neuroinflammation, mechanical strain, IL-1β, NLRP3 inflammasome, Sholl analysis, migration

Posted Date: April 21st, 2021

DOI: https://doi.org/10.21203/rs.3.rs-424697/v1

Title: Rapid morphologic and molecular activation of microglial cells by stimulation of the P2X7 receptor correlates with increased pressure and neuronal loss

Authors: Keith Campagno[1], Wennan Lu[1], Assraa Hassan Jassim[1], Farraj Albalawi[4,5,6], Aurora Cenaj[1], Huen-Yee Tso[1], Sophia P. Clark[1], Puttipong Sripinun[4] Néstor Más Gómez[1], Claire H. Mitchell[1-3]

Address: Departments of [1]Basic and Translational Science, Anatomy and Cell Biology, [2] Ophthalmology, [3]Physiology, [4]Orthodontics, University of Pennsylvania, Philadelphia, PA 19104; [5]Department of Preventive Dental Sciences, College of Dentistry, King Saud bin Abdulaziz University for Health Sciences, Riyadh, Saudi Arabia; [6]King Abdullah International Medical Research Center, Riyadh, Saudi Arabia

Corresponding Author: Dr. Claire H. Mitchell, Department of Basic and Translational Science, University of Pennsylvania, 240 S. 40th St, Philadelphia, PA 19104-6030 Tel: 215-573-2176 FAX: 215-573-2324 e-mail:chm@upenn.edu

Abstract

Background: The endogenous signals leading to microglial activation represent central components of neuroinflammatory cascades. Given ATP release accompanies mechanical strain to neural tissue, and the P2X7R for ATP is expressed on microglial cells, we examined the morphological and molecular consequences of P2X7R stimulation *in vivo* and *in vitro* in detail to enhance understanding of the response.

Methods: IL-1β release was determined with ELISA. Expression of mRNA used qPCR. ATP release was determined with the luciferin/luciferase assay while fura-2 indicated cytoplasmic calcium. Microglial migration used Boyden chambers. Morphological changes were quantified from Iba1-immunostained cells.

Results: Sholl analysis of Iba1-stained cells showed retraction of microglial ramifications one day after injection of P2X7R agonist BzATP into mouse retinae. Mean branch length also decreased, while cell body size and expression of *Nos2, Tnfa, Arg1, Chil3* increased. BzATP induced similar morphological changes in *ex vivo* tissue isolated from Cx3CR1-GFP mice, suggesting cell recruitment was unnecessary. Primary microglial cultures were developed to investigate the autonomous nature of the response. Isolated microglial cells expressed P2X7R, while increased intracellular Ca^{2+} triggered by BzATP and blocked by antagonist A839977 confirmed functional expression. BzATP induced process retraction and cell body enlargement within minutes in isolated microglial cells, and increased expression of *Nos2* and *Arg1*. BzATP both increased expression of IL-1β, and triggered a substantial release, suggesting P2X7R both primes and activates the NLRP3 inflammasome. ATP increased microglial migration, but this required

P2Y12R, not P2X7R involvement. As ATP release often accompanies mechanical strain, responses to intraocular pressure elevation were determined. Transient elevation increased ATP release and led to microglial process retraction, cell body enlargement and gene upregulation resembling the responses to BzATP injection. These pressure-dependent changes to microglia were reduced in P2X7R$^{-/-}$ mice. Critically, the loss of retinal ganglion cell neurons accompanying increased pressure was correlated with microglial activation in C57Bl/6J, but not P2X7R$^{-/-}$ mice.

Conclusions: P2X7R stimulation induced morphological and molecular markers of activation in retinal microglial cells *in vivo* and *in vitro*, affecting IL-1β release and rapid process retraction but not cell migration. Parallel responses accompanied transient pressure elevation, suggesting ATP release and P2X7R stimulation contribute to the microglial response to rising pressure.

Key Words

Microglial activation, P2X7 receptor, neuroinflammation, mechanical strain, IL-1β, NLRP3 inflammasome, Sholl analysis, migration

Introduction

Microglial cells are resident immune cells in neural tissue comprising 10-15% of neural tissue[1, 2], and are the primary cells of the central nervous system that are responsible for synaptic maintenance and innate immune response to injury or microbial infiltration [2, 3]. Dysregulation of microglia are implicated early events in several neuroinflammatory pathologies [4-6].

Microglia are fundamentally plastic, and undergo morphologic and molecular alterations when progressing from immunoquiescent, or M0, states into “activation” in response to exogenous triggers, accompanied by upregulation of microglial markers such as Iba1 [7] and CX3CR1 [8, 9]. While they are considered largely beneficial in their quiescent M0 state [10], stimulation leads to activation into a number of phenotypic states, depending on the nature of the specific activation trigger, simplified into classical activation (M1), or alternative activation (M2). Classical activation of microglia is defined by the release of proinflammatory cytokines or neurotoxic effectors, such as IL-1β or nitric oxide [11], respectively, and exacerbate neurotoxicity [12, 13]. Alternative activation has been demonstrated to promote neurogenesis [14, 15], axon remodeling [16], or remyelination [17] after an injury. An understanding of the varied effects of upstream regulators is important.

Changes in microglial morphology accompany activation states away from M0 neuroinflammation and cytokine release and have served as markers for neurodegenerative diseases [18, 19]. Immunoquiescent microglia have elongated processes and surveil their immediate environment [20] and interact with synapses [21]. Microglia demonstrate a diverse repertoire of morphological classifications [18, 22] but common morphologic alterations

observed with microglial activation include enlargement of soma size and reduction of branch length [23-25]. Phenotypic alterations have been associated with loss of neural populations in models of epilepsy [26, 27], traumatic injury [23], and stroke [24]. In glaucoma, microglial activation accompanied loss of retinal ganglion cells [28-30].

Extracellular ATP and the purinergic receptor P2X7 (P2X7R) have been identified as upstream effectors of microglial inflammation. ATP has been found in the parenchymal environment from mechanical perturbation [31-36], lysosomal exocytosis [37, 38], or cell death [39]. Once released, the extracellular ATP can stimulate ionotropic P2X or metabotropic P2Y receptors to mediate a response to the a number of stimuli. P2X7 is an nonselective ionotropic receptor stimulated with high millimolar ATP concentrations [28], and that is largely expressed on microglia within the central nervous system [40]. While a well-studied effect associated with P2X7 stimulation is release of master proinflammatory cytokine IL-1β via the NOD-, LRR- and pyrin domain-containing protein 3 (NLRP3) inflammasome, P2X7 receptor signaling is associated with a variety of intracellular processes [41-44], the accurate understanding of the effects of P2X7R stimulation on microglia morphological and molecular alterations associated with activation are understudied. Previous work on morphology within the retina has implicated adenosine receptor A_{2A} [45], or focused on the effects on P2X7R within microglia with elevated pressure [46-48] or *in vitro* stimulation [49] for extended periods of time. Herein, this study examines the morphological and molecular consequences of transient stimulation of P2X7 on microglia.

Materials and Methods

Animal care and use

All procedures were performed in strict accordance with the National Research Council's "Guide for the Care and Use of Laboratory Animals" and were approved by the University of Pennsylvania Institutional Animal Care and Use Committee (IACUC) in protocol #803584. All animals were housed in temperature-controlled rooms on a 12:12 light:dark cycle with food and water *ad libitum*. Mice (C57Bl/6J wild type and P2XR7$^{-/-}$ B6.129P2-P2rx7$^{tm1Gab/J}$ Pfizer and B6.129P2(Cg)-CX3CR1^{tm1Litt}/^{J} mice were obtained from Jackson Laboratories (Bar Harbor, ME). B6.129P2(Cg)-CX3CR1^{tm1Litt} $^{/J}$ mice were bred with C57BL/6J mice for pups that were heterozygous for GFP expression on the CX3CR1 promoter (CX3CR1$^{+/GFP}$). Long–Evans and Sprague Dawley rats were obtained from (Harlan Laboratories, Fredrick, MD).

Intravitreal injections

Intravitreal injections into C57Bl/6J mice as previously described [50]. Briefly, mice were anesthetized under 1.5% isofluorane and injected under a dissecting microscope using a micropipette attached to a microsyringe (Drummond Scientific Co., Broomall, PA, USA). The glass pipette entered the superior nasal region of the sclera into the vitreous cavity approximately 0.5 mm from the limbus. Total volume injected was 1.5 µl over 30 s. Injections consisted of Sterile Balanced Saline solution (as a control) with or without 250 µM Benzoylbenzoyl-ATP (BzATP, #B6396, Sigma Aldrich). The lens was carefully checked before processing the retinae and any eyes showing signs of lens damage were excluded from the study. For qPCR measurements, gene expression differences between saline-injected and naïve retinae from litter-controlled mates were not significant.

Immunohistochemistry

Mice were sacrificed and eyes removed. Dissected retinae were nicked to preserve orientation, incubated with 0.1% Triton X-100 in SuperBlock buffer (ThermoScientific, # 37515) for 30 minutes at 25°C and then blocked with 10% goat serum in SuperBlock for 1 hour. Retinal whole mounts or sections were incubated with Brn-3a (Santa Cruz Biotechnology, Inc. t# sc-31984, 1:250) and Iba1 (Wako Chemicals USA, Inc. # 019-19741, 1:500) overnight or Iba1 alone for 48 hrs at 5°C, followed by incubation with secondary antibodies; donkey anti-goat Alexa 555-conjugated antibody (#A21432, Invitrogen, 1:500) or donkey anti-mouse IgG Alexa Fluor 488 conjugated antibody (#A21202, Invitrogen, 1:500) for 60 min. Retinae were mounted with SlowFade Gold anti-fade mounting medium (#S36936, Molecular Probes). For cryosections used in Figure 5, sections were rinsed in PBS, blocked with (1% Triton X-100, 0.5% BSA, 0.9% NaCl, and 5% donkey serum [DKS; Jackson ImmunoResearch, West Grove, PA, USA] in 1% PBS; PBS-T-BSA), quenched using 0.3% H_2O_2, then incubated with Iba1 (Wako Chemicals USA, Inc. # 019-19741, 1:500) prepared in PBS-T-BSA for overnight (sections) at 4°C. Tissue and sections were rinsed in PBS then blocked in PBS-T-BSA. Secondary antibody Alexa-Fluor 568 (# A10042, Invitrogen, 1:250) prepared in PBS-T-BSA was added and incubated for 2 hours. DAPI (4',6-diamidino-2-phenylindole; 1:2000) was applied, then rinsed before sections were cover-slipped using Fluoromount-G (SouthernBiotech, Birmingham, AL, USA).

Image analysis

For retinal whole mounts subjected to saline or BzATP, Z-stacks were acquired from middle retina areas using a Leica TCS SP8 Confocal (Leica, Wetzlar, Germany) with 0.5 µm between z-planes, and central region, middle and peripheral retina regions defined as 0.2, 0.6 and 1.0 mm from the optic disk. Stacks were uploaded to FIJI [51] and processed to reduce background. Manual cell counting of the Retinal Ganglion Cell (RGC) and Inner Plexiform (IPL) layers were performed. For tracing or soma Iba1-intensity measurements, images were de-identified and cells were chosen randomly using *Randomizer.org* (www.randomizer.org). For retinal cryosections, images of non-peripheral retinal areas were acquired using a Nikon Eclipse microscope (Nikon, USA) and NIS Elements Imaging software (Nikon v. 4.60). All cells of the RGC and IPL layers were utilized for soma Iba1-intensity measurements. For Sholl analysis and summed branch measurements, Iba1-positive cells were manually traced using the FIJI Simple Neurite Tracer (SNT) plugin [52]. Sholl analysis was performed starting 5 µm from the center of the soma and analyzed every 1 µm thereafter. Iba1 soma intensity was measured in the z-stack using FIJI Measure plugin within a 5 µm ring centered at the soma and averaged from the z-stack at the peak fluorescence ± 1 µm (± 2 z-slices) in the z-plane to account for soma depth.

Quantitative PCR

Retinae or isolated microglia were homogenized using 1ml or 500 µl TRIzol reagent (#15596018, Invitrogen), respectively. RNA was purified using an RNeasy mini kit (#79254, Qiagen, Inc.). RNA concentration and purity were assayed using a Nanodrop spectrophotometer (Thermo Scientific). Conversion to cDNA was performed using the High Capacity cDNA Reverse Transcription Kit (#4368814, Applied Biosystems) at 25°C for 10 min, 37°C for 120 min and

terminated at 85 °C for 5 min. In most experiments, qPCR was performed with Power SYBR green (#4367659, Applied Biosystems) on the 7300 Real-Time PCR system (Applied Biosystems Corp.) using standard annealing and elongation protocols. For isolated microglia subjected to BzATP, Lipopolysaccharides (LPS, #L6529, Sigma-Aldrich), or Interleukin-4 (IL-4, #I1020, Sigma-Aldrich), expression was assayed using PowerUp Sybr Green (#A25742, Applied Biosystems) on the Quant Studio 3 Real-Time PCR system (Applied Biosystems Corp.) in Fast mode, again using standard annealing and elongation protocols. Data was analyzed using the delta-delta CT approach without conversion to RQ values as described [53]. Primers are listed in Figure S1.

Mouse retinal whole mount isolation

CX3CR1$^{+/GFP}$ mice were euthanized by CO_2. Eyes were enucleated and placed into isotonic solution. The cornea and iris were removed by cutting in a circular path along the ora serrata with small scissors while holding the eye at the limbus with a pair of forceps. The lens and vitreous humor weres removed, and the retina detached from the eyecup by cutting the optic nerve. 4 radial incisions were made, approximately 2/3 of the distance to the optic nerve, using spring scissors to create a butterfly shape. Retinae were briefly rinsed 3x with isotonic solution (consisting of 105 mM NaCl, 5 mM KCl, 6 mM 4-(2-hydroxyethyl)-1-piperazineethanesulfonic (HEPES) acid, 4 mM Na 4-(2-hydroxyethyl)-1-piperazineethanesulfonic acid, 5 mM $NaHCO_3$, 60 mM mannitol, 5 mM glucose, and 1.3 mM $CaCl_2$, pH 7.4) and incubated with or without 200 µM BzATP for 2 hours at 37° C. Retinae were then fixed with 4% PFA for 15 minutes at 25°C and mounted using SlowFade Gold anti-fade mounting medium (#S36936, Molecular Probes).

Primary cell cultures

Mouse microglial cell cultures: Primary retinal microglia were isolated from mouse pups of both sexes P12-P20 using standard methods [54, 55]. Briefly, eyes were enucleated and incubated in 3% dispase (#D4693, Sigma) in Hanks balanced saline solution without Ca^{2+}/Mg^{2+}. Retinae were removed and dissociated mechanically before growing on T75 flasks. Primary brain microglia were isolated along with retinal microglia for testing of microglia migration using published methods [56]. Brains were isolated, mechanically dissociated, and digested using 0.25% trypsin (#, Sigma) with 1 M HEPES buffer solution (#15630080, Thermo Fisher) in High Glucose Dulbecco's Modified Eagle Medium (HG-DMEM) for 30 min rocking at 37 C. Once finished, suspension was centrifuged at 500 x g and grown on T75 flasks with 3 brains per flask. In both cases, T75 flasks were pre-coated with Poly-L-Lysine (PLL, 0.01%, #OKK-3056, Peptides International) followed by Collagen IV (2 μg/ml, #354233, Corning) as described [57] and grown in HG-DMEM with 10% Fetal Bovine Serum (FBS), 1% Penicillin/Streptomycin (Pen/Strep, #15140122, Gibco), 1% GlutaMAX (#35050061, Gibco), and 1x MEM nonessential amino acids (#M7145, Sigma-Aldrich). Once cultures became confluent, microglia were "shaken off" manually and plated in dishes coated with 0.1% Poly-L-Lysine and Collagen IV (4 μg/ml). Microglial growth media contained DMEM plus 5% FBS, and 10% of media previously exposed to the mixed cell culture for 5-7 days. Cells grown without this preconditioned media showed lower rates of survival. Media was changed to DMEM containing only 5% FBS, 1% Pen/Strep, 1% GlutaMAX, and 1x MEM nonessential amino acids 24 hrs prior to experimentation.

Rat microglial cell cultures: Microglial cells were isolated from neonatal rat retinae using step 1 of the 2-step immunopanning protocol described previously [58]. In brief, retinae of Long Evans

rat pups PD 3-7 of both genders were dissected from each eye globe and dissociated for 30 min at 37°C in Hank's balanced salt solution (HBSS; Gibco, Inc. Invitrogen Corp., Carlsbad, CA) containing 15 U/mL papain, 0.2 mg/mL DL-cysteine and 0.004% DNase I. The retinae were washed and triturated in HBSS with 1.5 mg/mL ovomucoid, 1.5 mg/mL bovine serum albumin (BSA) and 0.004% DNase I, incubated with rabbit anti-rat macrophage antibody (10 min, 1:75, Accurate Chemical, Westbury, NY), centrifuged at 1000 rpm for 10 min, and washed. Cells were re-suspended in phosphate-buffered saline (PBS) containing 0.2 mg/mL BSA and 5 µg/mL insulin, and incubated for 15 min in a 100 mm Petri-dish coated with goat anti-rabbit IgG antibody (1:400, Jackson ImmunoResearch Inc, West Grove, PA). After shaking and washing to remove unattached cells, microglia were detached with 0.05% trypsin and cultured with growth medium (HG-DMEM containing 10% fetal bovine serum, 1% Pen/Strep, 1% GlutaMAX, and 1x MEM nonessential amino acids) on 6-well plates.

Rat astrocyte cultures: Primary cultures were grown from grown from optic nerve heads derived from Long-Evans rats as previously described [37]. In brief, rat pups of either gender were sacrificed by P5, and the optic nerve head digested for 1-2 hours with 0.25% trypsin (#25200056, Sigma-Aldrich). After trituration and washing, cells were grown in DMEM/F12, 10% FBS, 1% penicillin/streptomycin, and 25 ng/ml epidermal growth factor (#E4127, Sigma-Aldrich) on 35 mm culture dishes coated with PLL and grown at 37 C, 5.5% CO_2. Cells were determined to contain >99% GFAP-positive cells (#MABH360, Chemicon International Inc), defined as astrocytes.

Immunocytochemistry

Isolated retinal microglial cells were mounted on 12mm glass coverslips coated with PLL and collagen as above. Cells were fixed in 4% paraformaldehyde for 10 min at 37°C, washed in PBS with 1% Tween 20 (#170-6531, Bio-Rad), permeabilized with 0.1% Triton-X 100 for 15 min (#T8787, Sigma-Aldrich) then blocked with 20% Superblock (#37515, ThermoScientific) plus 10% goat or donkey serum. Primary antibodies against the following targets were used P2X7R (#APR-008, Alomone Labs, 1:200) then donkey anti-goat Alexa555 (#A21432, Invitrogen, 1:500); Iba1 (#AB48004, Abcam, 1:200) then donkey anti-rabbit Alexa488 (#A21206, Invitrogen, 1:500); Iba1 (#019-19741, Wako, 1:500) then goat anti-rabbit Alexa546 (#A11035, Invitrogen, 1:500) or donkey anti-rabbit Alexa555 (#A31572, Invitrogen, 1:500); GFAP (#MAB312 Chemicon, 1:500) followed by goat anti-mouse Alexa488 (#A11001, Invitrogen, 1:500) or donkey anti-rabbit Alexa555 (#A31572, Invitrogen, 1:500) and donkey anti-mouse Alexa488 conjugated antibody (#A11055, Invitrogen, 1:500); Synaptophysin (#MA5-14532, Invitrogen, 1:250) followed by donkey anti-goat Alexa555 (1:500). After incubation in Hoechst (#4082S, Cell Signaling, 1 µg/ml) for 10 min, coverslips were washed and mounted using SlowFade Gold anti-fade mounting medium (#S36936, ThermoFisher). Imaging was performed using a Nikon Eclipse microscope (Nikon, USA) and NIS Elements Imaging software (Nikon v. 4.60). ImageJ was used in parallel processing to modify intensity, and merge pseudocolored images.

Ca^{+2} imaging

Microglia were plated on 25mm coverslips that were coated with PLL 4 µg/ml Collagen IV and loaded with 10µM Fura-2 AM (#F1221, ThermoFisher) with 0.02% Pluronic F-127 (#P3000MP, Thermo Fisher) for 45min at 37°C. Cells were washed, mounted in a perfusion chamber, and

perfused with isotonic solution. Ratiometric measurements were performed using a 40x objective on a Nikon Diaphot microscope (Nikon, USA) by alternating excitation between 340nm and 380nm wavelengths and quantifying emission ≥512nm with a charge-couple device camera (All Photon Technologies International, USA) as described [59]. Data were expressed as the ratio of light excited at 340nm to 380nm, $F_{340/380}$, due to complexity of calibration. Statistical comparisons were made using the average of the final five measurements in each condition.

Time-lapse of morphological alterations

Retinal mouse microglia were plated as above and incubated in Mg^{2+}-free isotonic solution with 10 µM A839977 (#4232, Tocris) or DMSO as solvent control. Phase contrast images were taken every 12 or 15s using a Keyence BZ-X700 Series All-in-One Fluorescence Microscope (Keyence Corporation, Itasca IL). BzATP (#B6396, Sigma Aldrich) was added in the presence of A839977 or vehicle. Representative video was derived using "Focus tracking" function, where time-lapse video is comprised of best-focused images derived from a panel of 7 images spaced 0.7 µm apart at each time point. FIJI [51] was used to modify intensity, with parallel processing for all time-lapsed sequences.

Microglia migration

Microglia were grown to 80% confluence on a T75 flask and lifted with 0.25% trypsin, spun down at 500 x g and resuspended in media outlined above to a concentration of 50,000 cells in 390 µl. Cells were incubated in 1 µM A839977, 10 µM AR-C 69931 (#5720, Tocris), or vehicle for 1 hr, after which Hoechst nuclear dye (1 µg/ml) was added for 10 minutes. The cell suspension was

added to the top wells of a Boyden chamber (#AA96, Neuroprobe), separated from a solution of 1 mM ATP (#A2383, Sigma) in media by a 10 µm pore filter. Cells were allowed to migrate for 3 hrs, after which unmigrated cells were removed from the top of the filter. Filters were washed in PBS and fixed in 4% Paraformaldehyde in PBS, washed again, then imaged using the Lumoniskan Ascent fluorometer (ThermoFisher) at 340ex/527em. Values of background fluorescence were subtracted and conditions were normalized to control. To validate fluorescence measurements, images were acquired of labeled cells attached to the underside the pore filter and cells counted, with cell numbers compared to fluorescence measurements.

Intraocular pressure elevation

Transient elevation of IOP: A transient controlled elevation of IOP (CEI) procedure was produced in adult mice of both sexes using a modification of the approaches of Morrison [60] and Crowston [61] as described [62]. In brief, mice were deeply anesthetized with 1.5% isoflurane after receiving 2 mg/kg meloxicam. Proparacaine (0.5%) and tropicamide (0.5-1%) were administered and one eye was cannulated with a 30- gauge needle attached to polyethylene tubing (PE 50, #427411, Becton Dickinson, NJ) inserted into the anterior chamber, connected to a 20 ml syringe filled with sterile phosphate buffered saline (PBS). IOP was increased to 56.4 ±0.4 mmHg by elevating the reservoir to the appropriate height; blood flow through the retina was maintained throughout to avoid acute ischemia, although some reduction in blood flow is likely. After 4 hrs, IOP was returned to baseline, the needle removed and 0.5% erythromycin was applied to the cornea. The contralateral eye without cannulation served as a normotensive control. Retinal tissues were isolated 22-24 hrs after elevation of IOP.

Sustained elevation of IOP: Sustained elevation of IOP was induced using the microbead injection method. Ocular hypertension was mechanically induced in 2.5% isoflurane-anesthetized mice, using 2 µL of magnetic microbeads (COMPEL COOH-Modified 8-µm diameter, UMC4001; Bangs Laboratories, Fishers, IN, USA) injected into the anterior chamber of the eye using a glass-pulled micropipette connected to a manual microsyringe pump (World Precision Instruments, Sarasota, FL, USA) as described [63]. Magnetic beads were distributed along the trabecular meshwork using a neodymium magnet that draws them into the iridocorneal angle, allowing microbeads to block aqueous humor outflow through the trabecular meshwork. The resulting accumulation of aqueous humor causes an increase in IOP [64]. Both eyes were injected with beads to eliminate the confounding factor of contralateral eye effects on glial activation [65]. Separate mice injected with saline served as controls. This model proved reliable with minimum damage to ocular structures. Ten IOP measurements per eye of lightly isoflurane-anesthetized mice (2.5%) were taken and averaged; a baseline measurement was taken before bead injection, then weekly measurements after bead injection for 7 weeks using the TonoLab tonometer (Colonial Medical Supply Co, Londonderry, NH). The IOP integral (mm Hg-days exposure over baseline) was calculated to quantify cumulative IOP elevation [63]. Fixed retinae were cryoprotected in 30% sucrose and 0.02% sodium azide in 0.1M PBS and embedded in optimal cutting temperature medium for sagittal at 10 to 15 µm using a Leica cryostat. Six to ten representative slides (three-four sections/slide) were imaged. Images were captured using a Nikon Eclipse microscope (Nikon, USA). Mean intensity of Iba1 in microglia soma were analyzed using four sections per slide, and ten slides per retina using Image J. Data was derived from the central regions of the retina, consistent with above methods of intensity measurements.

311

312 *Vitreal ATP measurement*

313 ATP was determined by fast-freezing the eye as soon as IOP returned to baseline, then dissecting
314 the eye over dry ice, and collecting vitreal samples by chipping away frozen samples. This
315 prevented intracellular ATP from the cut tissue edges from seeping into the vitreous and
316 contaminating the sample [32]. ATP levels were measured using the luciferin/luciferase assay
317 (Sigma-Aldrich Inc.) as described [32].

318

319 *Observer quantification of morphological alterations*

320 Retinal whole mount images were acquired using a Nikon Eclipse microscope (Nikon, USA), and
321 images collected from the central, middle, and peripheral regions of the retina as defined above,
322 with images taken from the superior, nasal, inferior, and temporal quadrants at each distance
323 from the optic nerve. Images were de-identified and scored individually based upon morphology,
324 with smaller cell body size and elongated, thin processes receiving a score of 1 and larger body
325 size and short, thick processes receiving a score of 3 (Fig. S3A, C). Methods were validated by
326 correlating observer scoring of BzATP-exposed retinae to Iba1-intensity of the soma region (Fig.
327 S3B). There was close agreement between different observers, with the standard deviation of
328 the scores between observers being less than 15% of the mean across all regions, validating the
329 approach.

330

331 *Cytokine measurement*

For mouse experiments, isolated microglial cells were isolated and replated using the shake-off method as outlined above, and subsequently primed with 1 μg/ml lipopolysaccharides (LPS, #L6529, Sigma-Aldrich) prior to exposure to agonist. IL-1β was measured using the either the Mouse IL-1 beta/IL-1F2 Quantikine ELISA kit (#MLB00C, R&D Systems) following the manufacturer's instructions, with minor alterations. Briefly, supernatants were removed and spun down at 500 x g to remove cell debris. Samples, standards, and controls were added to microplate and allowed to bind overnight at 4 C. Washes, substrate solution, and stop solution were added as outlined. Optical density was measured at 450 nm with subtraction of 540 nm measurements using the SpectraMax ABS (Molecular Devices). Values were converted back into absolute amounts using the standard curve. Due to the high variability between experiments, experimental conditions were normalized. IL-1β from rat microglial cells and astrocytes were primed with 500 ng/ml LPS and rat Interleukin-alpha (IL-1α, #500RL-005, R&D Systems) followed by exposure to agonist. IL-1β was measured using the Rat IL-1 beta/IL-1F2 Quantikine ELISA Kit (#RLB00, R&D Systems) following the manufacturer's instructions.

Data analysis

Data are displayed as mean ± standard error of the mean. Statistical analysis was performed using GraphPad Prism software version 9.0.0 (Graphpad Software, Inc. San Diego Ca, USA). Normality of data was tested using the Shapiro-Wilk test. Significant differences between two groups were assessed by Student's t-test; paired Student's t-tests employed when making 1:1 comparisons. For comparisons among three groups, one-way analysis of variance (ANOVA) with Dunnet's multiple comparison's test. For comparisons among four groups, two-way ANOVA followed by

Tukey's multiple comparison's test or was applied. For quantification of calcium imaging or Sholl analysis, One-way or Two-way ANOVA with Repeated measures with Sidak's test for multiple comparison's was used, respectively. Results returning $p<0.05$ were considered significant.

Results

P2X7 receptor stimulation leads to morphologic and molecular activation of microglia in vivo.

The response of microglial cells *in vivo* to the P2X7 receptor agonist BzATP was investigated to determine whether stimulation of the P2X7 receptor was sufficient to evoke morphologic changes. BzATP (250 μM) or saline control was injected intravitreally into eyes of C57Bl/6J mice, and retinae removed after 24 hours. Treatment with BzATP led to elevated Iba1 staining and retracted microglial processes, consistent with microglial activation (Fig. 1a-d) [6,7]. Microglia reside primarily in the Retinal Ganglion Cell Layer (RGCL) Inner Plexiform Layer (IPL), and the Outer Plexiform Layer (OPL) of the retina, where they maintain homeostasis near synapses [66, 67]. The elevated Iba1 immunoreactivity following BzATP injection was observed mainly in the RGCL and IPL (Fig. 1c, d).

To quantify the extent of process retraction induced by P2X7 receptor stimulation, images were traced to produce binary outputs, and Sholl analysis was performed (Fig. 1e) [24]. Retinal BzATP exposure led to a significant reduction in microglial process length and complexity compared to saline controls (Fig. 1f). Furthermore, the cumulative length of all branches was reduced (Fig 1g), representing a reduction in summed process length (Fig. S2). Iba1 intensity was measured in a defined area (5 μm) encircling the microglial soma in randomly selected microglia

from saline- or BzATP-injected eyes (Fig. 1h, I). Exposure to BzATP led to a significant elevation of Iba1 immunostaining intensity when compared to control counterparts (Fig. 1j), reflecting a combination of increased soma size and Iba1 expression. Evaluation of changes to microglial morphology based on Iba1 intensity and process retraction by masked observers found consistent signs of activation in retinae exposed to BzATP (Fig. 1k, S3).

Microglia display a variety of molecular gene-expression states in response to insult or injury; these are traditionally characterized into classical activation and alternative activation, with classical activation (M1) broadly associated with a pro-inflammatory state, and alternative activation (M2) promote neural repair [11, 16, 18, 68-70]**,** although cell states are now recognized as being more fluid and less binary [2, 71-73]. To evaluate the changes in gene expression accompanying P2X7 receptor stimulation, qPCR was performed on retinal tissue; genes associated with classical activation, *Nos2* and *Tnfa*, and genes associated with the alternative activation state, *Arg1* and *Chil3*, were elevated in retinae 24 hours after *in vivo* exposure to BzATP (Fig. 1l). Together, the morphological and molecular changes are consistent with microglial activation in response to P2X7R stimulation.

The response of microglial cells in isolated retinal whole mounts to agonist BzATP was examined to determine if resident microglia were sufficient for observed alterations in morphology following P2X7 receptor stimulation. The use of an *ex vivo* retinal whole mount restricted the response to microglial cells already present in the retina. Retinal whole mounts derived from heterogeneous mice with a fluorescent tag attached to microglia/macrophage receptor $CX3CR1^{+/GFP}$ were used to track the response most effectively. Retinal whole mounts were placed in a petri dish and BzATP (200 μM) was added for 2 hours. Exposure to BzATP led to

a considerable increase in fluorescence, with morphological changes resembling those observed after BzATP injection. The increased signal was most noticeable around the optic nerve head (Fig. 2a, b), with prominent cell bodies apparent. Exposure to BzATP also increased the signal throughout the central (Fig. 2c, d) and peripheral retina, and across retinal layers (Fig. 2 e, f). This *ex vivo* response in isolated retina suggests that microglia normally resident within the retina are capable of responding to P2X7 receptor stimulation, although it cannot rule out recruitment of additional monocytes, which occurs *in vivo*.

P2X7 receptor stimulation leads to morphologic and molecular activation of isolated microglial cells

Isolated retinal microglia were examined to determine whether stimulation of the P2X7 receptor could induce effects on microglial cells directly. Dissociated retina and brain tissue were cultured in conditions that preferentially supported survival of glial cells; the microglial cells growing on top of the cultures were collected using the shake-off method [55, 56, 74]. The relative staining for Iba1 and astrocyte marker GFAP, and neural marker synaptophysin suggested preparations contained >95% microglial cells (Fig. 3a).

To support the microglial identity of the cells, the ability of lipopolysaccharides (LPS) and interleukin-4 (IL-4) to induce expression of activation state markers was determined using qPCR, as these two agonists are traditionally associated with classical and alternative activation states, respectively [11, 75]. 4-hour stimulation of isolated retinal microglial cells with LPS (10 ng/ml) increased expression of *Nos2, Tnf,* and *Il1b*, while stimulation with IL-4 (10 ng/ml) increased expression of markers for the alternative activation state such as *Chil3* and *Arg1* (Fig. 3b). These

responses suggest cells cultured under these conditions responded as expected for microglial cells.

Immunocytochemistry staining indicated Iba1-positive cells expressed the P2X7 receptor, supporting the presence of the receptor on these primary microglial cultures (Fig. 3c). Functional expression of the P2X7 receptor on isolated retinal microglial cells was assessed by examining levels of cytoplasmic Ca^{2+} with the ratiometric indicator Fura-2. A brief, 1 minute addition of BzATP (100 µM) raised cytoplasmic Ca^{2+} in the microglial cells (Fig. 3d, e); the response was rapid, with most cells showing a response within 20 sec. The response was also reversible upon wash-out of BzATP, and repeatable upon reapplication; these characteristics are consistent with an ionotropic channel with little inactivation like the P2X7 receptor and have been observed previously [76]. The P2X7R-specific inhibitor A839977 [77] significantly reduced the Ca^{2+} rise triggered by BzATP, with the response to BzATP evident after removal of the A839977 confirming this decrease was not due to Fura-2 depletion (Fig 3d, e). Together this supports the functional presence of P2X7 receptors on these isolated retinal microglial cells.

The effect of BzATP on microglial morphology was examined next. BzATP triggered a retraction of microglial processes and a rounding of the cell body (Fig. 4a, S3) in greater than 75% of observed cells. This response was rapid, starting less than 7 minutes after BzATP application (Fig. S4). The effect of BzATP on microglial morphology was greatly reduced or inhibited in the presence of inhibitor A839977, supporting action at the P2X7 receptor. This suggests that stimulation of the P2X7 receptor was sufficient to trigger the morphological changes seen *in vivo*, and that these changes occurred rapidly. Stimulation of the P2X7 receptor on isolated microglial cells also induced changes in gene expression with parallels to those observed *in vivo* after P2X7

receptor stimulation. Specifically, the endogenous agonist ATP (Fig. 4b), and P2X7 receptor agonist BzATP (Fig. 4c) both increased expression of *Nos2* and *Arg1*.

Stimulation of purinergic receptor P2Y12 has been shown to trigger microglial migration up a purinergic gradient. This was tested in isolated retinal microglial cells using a 2-part Boyden Chamber across a filter. Initial measurements indicated that the number of Hoechst-stained microglial cells was closely reflected by total Hoechst fluorescence (Fig. 4d, e). Subsequent imaging of the filter with bound microglia confirmed elevated migration by retinal microglia towards an ATP concentration gradient (1 mM) (Fig. 4f). Migration levels were optimal 3 hours after the addition of cells to the chamber. This migration was inhibited with exposure to P2Y12 inhibitor AR-C 69931 (100 µM), but not P2X7 inhibitor A839977 (10 µM) (Fig. 4f). These data lend support to *in vivo* results of microglial-specific activation following injection of BzATP, without the need for peripheral migration.

Role of ATP and the P2X7 receptor in pressure-dependent microglial activation

The effect of IOP elevation on microglial cells was examined. The mechanosensitive release of ATP is one of the earliest events found after pressure elevation in rat and bovine eyes, and remains elevated in mouse, rat and primate models of sustained IOP elevation [32, 33, 62]. To confirm short-term changes in IOP induced a rise in extracellular ATP, the transient CEI procedure was used to elevate IOP for 4 hrs, and ATP concentration was determined as soon as pressure returned to baseline. Given the difficulties in sampling the small extracellular spaces in the retina without touching cells to trigger mechanosensitive ATP release or rupturing cells to trigger cytoplasmic ATP release, levels in the posterior vitreous were determined. The fast-frozen

approach was used to prevent ATP from cut edges seeming into the vitreal chamber, as described previously [32]. ATP levels sampled in the vitreal humor near the inner limiting membrane were significantly elevated in eyes subjected to increased IOP as compared to normotensive controls (Fig. 5a).

Previous studies have indicated that inflammatory responses were greater when examined one day after IOP was returned to baseline [62], thus retinae were examined 22-24 hours after return of IOP to baseline after this 4 hr elevation of IOP using the CEI procedure. Staining of retinal whole-mounts for Iba1 revealed a noticeable change in microglial morphology in eyes exposed to elevated IOP, with larger cell bodies and shorter processes in retinal tissue exposed to elevated IOP as compared to control (Fig. 5b, c). Changes in microglial morphology were quantified across Central and Middle retinal regions, excluding peripheral regions for divergent cell ratios (Fig. S5a, b). Analysis indicated a clear increase in morphological signs of activation in microglial cells following IOP elevation (Fig. 5d). Similar morphological differences were observed in the central regions of the retinae from C57Bl/6J mice subjected to sustained elevation of IOP via magnetic bead blockage of aqueous humor outflow (Fig. 5e, f). Iba1 staining revealed morphological retraction of processes, cell soma swelling, and increased expression of Iba1 when compared to saline-administered retinae (Fig. 5g, h). Quantification of Iba1 intensity in the soma area was significantly elevated with increased IOP (Fig. 5i). Furthermore, the elevation of IOP utilizing this method reinforces data that were derived using transient elevation of IOP.

To evaluate the changes in gene expression accompanying the increase in IOP, qPCR was performed on retinal tissue; levels were examined one day after IOP elevation as previous work

indicated expression changes peaked at this point [62]. As with retinal BzATP-injection, genes associated with classical activation, *Nos2* and *Tnfa*, and genes associated with the alternative activation state, *Arg1* and *Chil3*, were elevated (Fig. 5j). Expression of *Lcn2*, the gene coding for inflammatory marker lipocalin 2, was also increased in the model; lipocalin 2 expression is increased in microglial cells exposed to inflammatory stimuli [78] and is upregulated in retinal microglial cells [79], and is increased early in humans with glaucoma [80], although expression is also associated with reactive astrocytes in optic neuritis [81]. Together, the morphological and molecular changes are consistent with microglial activation in response to transient pressure elevation.

To determine whether the P2X7 receptor contributed to the microglial responses to elevated IOP, the degree of morphological and molecular change was compared between P2X7R$^{-/-}$ and C57Bl/6J mice. Microglial in the retinae of P2X7R$^{-/-}$ mice displayed a smaller change in morphology after exposure to transient IOP elevation (Fig. 6a, b). Histological quantification confirmed that changes in microglial morphology were largely absent in retina from P2X7R$^{-/-}$ mice (Fig. 6c).

Further analysis was performed to better understand the reasons for the difference between wild type and P2X7R$^{-/-}$ mice. Microglial cells in normotensive retina from P2X7R$^{-/-}$ mice showed a small increase in morphological activation as compared to normotensive retina from wild type mice (Fig. 6d). In contrast, the morphological changes after IOP elevation were significantly less in retina from P2X7R$^{-/-}$ mice (Fig. 6e). Together this implies that the lack of an IOP-induced change in microglial morphology in retina from P2X7R$^{-/-}$ mice is due to both a smaller response to increased pressure itself and a moderate increase in baseline scores.

The expression of genes associated with non-M0 microglial states increased in retina of P2X7R$^{-/-}$ mice after exposure to elevated IOP, but the rise was smaller and results were variable. The expression of genes *Tnfa*, *Arg1* and *Lcn2* increased in retina of P2X7R$^{-/-}$ mice after exposure to elevated IOP, but the rise was smaller and there was no significant change in *Nos2* or *Chil3* expression (Fig. 6f). Overall, the change in expression of genes following IOP elevation was reduced in retina from P2X7R$^{i-/-}$ mice as compared to C57Bl/6J mice (Fig. 6g), although changes in each gene were inconsistent.

Stimulation of the P2X7 receptor upregulates Il1b gene expression and IL-1β cytokine release.

Cytokine IL-1β is implicated in neuroinflammation and death of neuronal populations [13]. To examine the neuroinflammatory components of P2X7 receptor stimulation, cytokine release from cultured mouse retinal microglia was determined. Retinal microglial cells primed with LPS (1 μg/ml) and exposed to ATP (3 mM) (Fig. 7a) or BzATP (200 μM) (Fig. 7b) secreted more IL-1β protein than LPS alone, and this was inhibited by P2X7 receptor antagonist A839977 (1 μM). *Il1b* gene expression was also upregulated in cultured microglia that were challenged with ATP (1 mM) for 4 hours (Fig. 7c), indicating "priming". A similar increase in *Il1b* expression was found *in vivo* in retinae 24 hours after transient elevation of intraocular pressure as compared to normotensive controls in both C57Bl/6J mice and P2X7R$^{-/-}$ mice, although this rise in *IL1b* expression was significantly less in P2X7 mice than in C57Bl/6J mice (Fig. 7d).

To compare the relative IL-1β release in microglia and astrocytes, material from rat eyes was used to take advantage of available primary cultures of optic nerve head astrocytes. The

amount of IL-1β released from microglial cells was substantially greater than that released from astrocytes when both were primed and exposed to 3 mM ATP (Fig. 7e). Taken together, P2X7 receptor stimulation results in gene upregulation and release of IL-1β in microglial cells.

Retinal ganglion cell loss, microglial activation and the P2X7 receptor

The final set of experiments examined the relationship between retinal ganglion cell loss, microglial activation and the P2X7 receptor. Retinal whole mounts used above were co-stained for the ganglion cell transcription factor Brn3a and the number of cells present in each region were counted in a masked fashion. In C57Bl/6J mice, IOP elevation led to a modest reduction in the number of Brn3a-positive cells as compared to normotensive eyes (Fig. 8a). Little change in retinal ganglion cell number was apparent when IOP was elevated in $P2RX7^{-/-}$ mice (Fig. 8b). Quantification of Brn3a-positive cells indicated cell loss accompanying elevation of IOP in C57Bl/6J mice (Fig. 8c). In contrast, no reduction in retinal ganglion cell number was found in $P2RX7^{-/-}$ mice (Fig. 8c). Close overlap between microglial cells and retinal ganglion cells occurs throughout the retina (Fig. 8d). To determine whether the magnitude of microglial activation was associated with retinal ganglion cell loss in retinae stained for both Brn3a and Iba1, the % of ganglion cell loss was plotted against the % rise in microglial activation score for each image. There was a loose but significant correlation between ganglion cell loss and microglial activation in the C57Bl/6J mice (Fig. 8e), but not in the $P2RX7^{-/-}$ mice (Fig. 8f) suggesting that microglia activation may negatively influence loss of RGCs.

Discussion

548 The data presented in this manuscript illustrate several complex consequences of P2X7
549 receptor activation in microglial cells. Administration of P2X7 receptor agonist BzATP to mice
550 retina resulted in reduction of branch length, and increase in soma size and Iba1 expression in
551 microglial cells, emblematic of microglia activation. Furthermore, retinae exposure to BzATP
552 resulted in gene expression upregulation of *Nos2, Tnfa, Arg1,* and *Chil3*, which are associated
553 with microglial activation into a mixed M1/M2 state. *In vitro* data demonstrated comparable
554 morphological changes following exposure to BzATP, or molecular changes after exposure to ATP
555 or BzATP, with subsequent upregulation of M1 marker *Nos2* and M2 marker *Arg1* observed 4
556 hours after exposure. Finally, transient elevation of intraocular pressure resulted in similar
557 reduction in process length and complexity observed in Iba1+ cells, as well as gene expression
558 changes similar to those in retinae observed with administration of BzATP. These morphological
559 and gene expression changes were significantly reduced in retinae from $P2X7R^{-/-}$ mice subjected
560 to transient elevation of IOP. Given the parallels in morphological and molecular changes from
561 agonist-dependent stimulation and from elevated pressure, as well as the differences observed
562 in $P2X7^{-/-}$ mice, these results implicate the P2X7 receptor in some of the early inflammatory
563 responses to pressure in the retina.
564
565 *Microglial activation as an early event in retinal degeneration.*
566 Microglial activation has been implicated as an early event in the DBA/2J model of
567 glaucoma [6], or chronic ocular hypertension (COH) in rats [47, 82]. Furthermore, previous work
568 in rats demonstrated microglial activation 3 days after comparatively high concentrations of
569 BzATP [47]. The work presented here demonstrated microglial activation observed after 24 hours

of BzATP administration (Fig. 1) or elevation of intraocular pressure for 4 hours (Figs. 5, 6) and indicated that the time scale is earlier than reported elsewhere. Our study confirms the likelihood of a direct effect of microglial P2X7 receptor stimulation on morphology, given that immune cells express P2X7 at a higher concentration than other cell types [40, 83]. Furthermore, rat P2X7 reactivity to BzATP is significantly a pEC_{50} of 5 versus 4 in mouse [84, 85], and single nucleotide polymorphism differences between mouse strains altering receptor pharmacology [85, 86]. Finally, the discovery that $_{P2X7}$ receptor stimulation can induce cell proliferation, plus the notion that tumor or inflammatory microenvironments may tonically stimulate the P2X7 receptor without inducing cell death places, value on understanding the effects of submaximal $P2X_7$ receptor stimulation [87]. Taken together, administration of a submaximal dose of BzATP resulted in early activation of microglia, and points to P2X7 signaling as upstream to microglial activation.

P2X7 receptor stimulation results in mixed activation state.

The data presented herein add to the growing body of evidence that the molecular response to transient $P2X_7$ stimulation cannot be strictly categorized to M1 or M2-like cell state. *In vivo* administration of BzATP or elevation of IOP resulted in retinal gene upregulation of both M1 markers 4-hour stimulation of the P2X7 receptor in cultured microglia with 1 mM ATP or 200 µM BzATP resulted in upregulation of M1 gene marker *Nos2* and M2 gene marker *Arg1* (Fig. 4b, c), paralleling *Nos2* and *Tnfa* and also M2 markers *Arg1* and *Chil3* observed with *in vivo* administration of BzATP, or elevation of IOP (Fig. 1l; Fig. 5j). Stimulation of the P2X7 receptor had been shown to lead to upregulation of M1 markers in in a variety of inflammatory cell types [41,

88, 89], with stimulation often associated with the activation step of the NLRP3 inflammasome and subsequent release of IL-1β, widely considered to be a proinflammatory (M1) cytokine [11]. Previous studies utilizing acute elevation of IOP in rats have focused on neurotoxic cytokine release without examination of potential compensatory release of neuroprotective factors [48]. However, 15-minute stimulation of the P2X7 receptor has been demonstrated to elevate protein expression of M2 markers Arg1 and CD163 in the SOD1-G93A mouse model of Amyotrophic Lateral Sclerosis [90], correlating with a brief induction of autophagy [44]. This suggests that transient stimulation of the P2X7 receptor may promote a mixed activation state, consistent with phenotypic state being a complex matter [73, 75, 91]. Influencing the microglia state has been suggested as therapeutic for conditions of brain trauma that are accompanied with transient elevated ATP [16, 68, 69]. Furthermore, localization to general retinal areas, or near to degenerating RGCs may provide information correlating state of activation with effects on retinal degeneration. The correlation between regions of greatest microglial activation with RGC loss in the present study emphasize this elationship, but data do not alllow us to distinguish between microglial activation in response to dying neurons or neurons dying in response to microglial activation; distinguishing between these is of key furure interest..

NF-κB signaling is a well-known effector in the expression of inflammatory cytokines [89][91][92], and is implicated in polarization to the M1 phenotype [93, 94], which was confirmed in our exposure to upstream effector LPS/TLR4 to induce an M1 phenotype (Fig. 3b). Previous work has indicated that P2X7 stimulation alone can lead to NF-κB translocation to the nucleus via MyD88 [62, 95]. Modulation of NF-κB has also been demonstrated to enhance microglial

polarization to the M2 phenotype, with has demonstrated benefits in models of spinal cord injury [96] and cerebral ischemic injury [93].

Morphological alterations with P2X7 receptor stimulation.

The intracellular and extracellular mechanisms leading to microglia activation have yet to be deduced. Brief P2X7R stimulation *in vitro* resulted in morphological changes and expression of M1/M2 markers (Fig. 4). HEK293 cells exposed to brief P2X7 stimulation with 100 µM BzATP resulted in actin reorganization in a process dubbed "pseudoapoptosis", with demonstrable membrane blebbing and mitochondrial swelling, and the process was largely dependent upon Ca^{2+} influx and ROCK-1 signaling [97]. In the current study, *in vitro* microglia were exposed to 200 µM BzATP for ten minutes and demonstrated no signs of membrane blebbing (Fig. 4a, Sup Fig. 4). However, these morphological changes were absent after incubation with Calcein-AM, which binds calcium, acting effectively as a chelator (data not shown). One downstream possibility was demonstrated in the BV2 microglial cell line, where LPS-induced morphological changes were ablated with caspase 3/7 inhibition [98]. P2X7 receptor stimulation activates caspase-3 in rat cortical neurons [99] and the J774 macrophage cell line in the context of inducing apoptosis [100], but the role of calcium influx in the process is not known.

While changes to microglia morphology and expression of markers *in vitro* paralleled those expressed *in vivo*, these experiments were conducted in the absence of factors that promote immunoquiescence, such as Cx3CL1/Cx3CR1, or CD200/CD200R interactions. Cx3CR1 in the CNS is present largely on microglia [101, 102]. Elimination of the receptor elevated microglial activation after elevation of IOP [103] and promoted inflammatory cytokine expression,

increased pro-inflammatory activation, and increased phagocytosis of photoreceptors in the rd1 mouse model of Retinitis Pigmentosa [104]. Furthermore, Cx3CR1-deficient mononuclear phagocytes expressed higher levels of P2X7 receptor than their wildtype counterparts [105]. Exogenous administration of the Cx3CR1 ligand Cx3CL1 (fractalkine) reduced activation and phagocytosis by activated microglia [104]. Similar results were observed with CD200R blockade leading to increased activation and IL-6 and Nos2 protein expression in rat spinal macrophages, and to worse outcomes in a multiple sclerosis model [106]. In neuroinflammatory diseases such as Alzheimer's diseases, promotion of Cx3CLR1 signaling has been demonstrated to be beneficial in reducing disease progression [107]. Interestingly, Cx3CR1 expression appears to be upregulated in microglia that have been activated with P2X7 receptor stimulation (Fig. 2), indicating that concurrent examination of factors that promote immunoquiescence may provide a fruitful direction concurrent to understanding P2X7-mediated inflammation.

P2X7-mediate microglial activation effect on RGC degeneration.

Microglial activation is likely to have both positive and negative consequences following the elevation of ocular pressure. The correlation between activation and the loss of retinal ganglion cells suggests activation can lead to neuronal death, but it is possible the relationship goes the other way, and the loss of ganglion cells contributes to microglial activation [10]. Likewise, while it is tempting to assume that the lack of a correlation between microglial activation and neuron loss in the $P2X7R^{-/-}$ mouse reflects receptor role in microglial activation, the P2X7 receptor is also expressed on retinal ganglion cells and BzATP can kill isolated ganglion cells [108]. Thus the causal direction of this correlation awaits cell specific knockdown of the P2X7

receptor. The levels of pressure attained in the transient IOP elevation studies are just at the point where damage is observed; while this is considerably above the pressures observed in most common forms of glaucoma, the presence of microglial activation in a model of sustained moderate IOP suggests there is value in the model.

The morphologic and molecular changes observed in response to transient elevation of IOP suggest microglial activation is certainly one of the earliest responses to IOP elevation. In the DBA/2J mouse model of chronic glaucoma, morphological changes to microglial cells were reported at 3 months of age, long before most markers of neural damage were detected [6]. The transient controlled elevation of IOP model used in this study enables precise control over the timing of pressure change, making it ideal for examining the kinetics of cellular responses [60, 61]. Examination at earlier time points may indicate whether microglial activation precedes neuron loss *in vivo*. However, the rapid retraction of microglial ramifications exposed to BzATP *in vitro* suggests changes to microglial morphology occur soon after P2X7 receptor stimulation. Studies using the chronic ocular hypertension model in rats support this correlation [47, 48] but did not address microglia cell state or to define any spatial correlation between activation and RGC loss. Related studies have focused on associated mechanisms, such as alterations to purinergic receptor expression [109], or general activation of the NLRP3 inflammasome [110]. However, the current study identifies a clear role for the P2X7 receptor in morphological and molecular changes in retinae.

Microglia activation correlated spatially to loss of RGCs, and this correlation was absent in retinae from P2X7R$^{-/-}$ mice. (Fig. 8). These data suggest P2X7 is responsible for a local inflammatory response. This idea agrees with the high millimolar concentration of ATP required

679 to activate the P2X7 receptor [86, 111]. Whether RGC death and the subsequent release of ATP
680 is upstream of P2X7 receptor signaling, or microglial activation mediated via P2X7 receptor is a
681 contributing factor, needs to be examined. Recently, work has pointed to complex intercellular
682 signaling pathway between neurons, microglia, and astrocytes leading to neuronal cell death
683 [112-114]. Interestingly, IL-18, a product of NLRP3 inflammasome activation, has been
684 demonstrated to induce the A1 astrocyte phenotype, and the inhibition of NLRP3 inflammasome
685 signaling with NLRP3-inhibitor MCC-950 has been demonstrated to reduce it [114].

686 Recent work has indicated that removal of the P2X7 receptor negatively effects on RGC
687 function three days after 30 min elevation of IOP [115]. The difference between Wang et al, and
688 our current study may be reflected in the difference of time of elevated pressure, the focus on
689 RGCs rather than microglia, or the focus on use of microelectrode arrays to study RGC function,
690 which may compromise the effects of cytokines released. Even so, P2X7 receptor stimulation has
691 been demonstrated to have a number of neuroprotective effects in neuronal models [58, 116]
692 even though stimulation often favors cell death [108]. The use of *in vivo* models with prolonged
693 elevation of IOP [110] complicates the effect on RGCs, with P2X7 stimulation of microglia leading
694 to RGC death [110], yet IL-1β release (a major effect of P2X7 receptor stimulation [117]) has been
695 demonstrated to protect RGCs from excitotoxic damage after exposure to NMDA [118]. These
696 observations stress the need for an open mind when distinguishing between the physiologic and
697 pathophysiologic contributions of the P2X7 receptor, and stress that small differences in models,
698 such as absolute intraocular pressure levels, may influence the outcome.

699

700 *IL-1*β *upregulation and release with P2X7 receptor stimulation*

Stimulation of P2X7 with high concentrations of ATP resulted in elevation of *Il1b* mRNA in retinae and in isolated microglia, and release of the protein product from LPS-primed isolated microglia (Fig. 7). IL-1β has been traditionally termed a master cytokine, and has been demonstrated to contribute to neuroinflammatory diseases [13] and influence the microglia inflammatory state [119]. However, IL-1β/IL-1R signaling in microglia needs further exploration. IL-1R has been shown to be minimally expressed in microglia [118, 120]. Yet interestingly, IL-1β released with concurrent P2X7 pore opening promoted microglia proliferation [117] possibly via crosstalk with astrocytes [118] or endothelial cells [121]. Microglia are likely sources of IL-1β release, as astrocytes do not release much IL-1β themselves, as confirmed in Fig. 7e [62]. Specific signaling needs to be determined, however. IL-1β released from microglia has reduced excitotoxic neuron loss [118]. Concurrent release of IL-1β with P2X7 receptor stimulation *in vitro* points to downstream neurotoxic factors that may contribute to neuron loss. The role of RGC loss from elevated IOP was not observed in mice where *IL1α*, *TNFα*, and *C1q* were knocked out [112, 114], and the role of IL-1β as either a factor contributing to or protecting against neural toxicity, and stimulating neurons directly, or altering microglia dynamics via crosstalk with other cell types, needs to be elucidated. P2X7 antagonism is a promising target for several neuroinflammatory diseases, but antagonism may have unintended effects of disrupting neuroprotective mediators concurrent with M2-like signaling depending on the time course.

Microglia/neuron crosstalk is complex and mediated by local extensions to synapses [21]. Reduction of microglia dendrites as an early event to transient, submaximal P2X7 stimulation may contribute to reduced RGC function and toxicity via loss of local secretion of neuroprotective

factors. Careful local examination of protein expression may lead to novel therapies for RGC protection in diseases of elevated ATP or pressure.

Conclusion

In summary, our results support a model where P2X7 receptor stimulation alone is sufficient to cause microglial activation, and that this activation occurs very rapidly after receptor stimulation or elevation of intraocular pressure. Furthermore, although the P2X7 receptor is traditionally associated with its proinflammatory role [41], P2X7 receptor stimulation led to a mixed activation state in microglial cells, suggesting the response is complex. IL-1β cell upregulation was demonstrated under a number of conditions suggestive of P2X7 receptor fulfilling both the priming and the activation step of NLRP3-inflammasome signaling. The effector signaling of the IL-1β, as well as the nature of the mixed M1/M2 activation state with any associated M2 factors needs to be determined. As P2X7 receptor modulation is being targeted for retinal disorders [122], this study and subsequent work can add to a deeper understanding of P2X7 receptor signaling and putative beneficial effects.

Declarations

Abbreviations: ATP: Adenosine triphosphate; BzATP: Benzoylbenzoyl-ATP; Ctrl: Control; Cx3CR1: CX3C chemokine receptor 1; ELISA: Enzyme-linked immunosorbent assay; GFAP: Glial fibrillary acidic protein; Iba1: ionized calcium-binding adapter molecule 1; IL-1β: Interleukin 1 β; IL-4: Interleukin 4; IPL: Inner plexiform layer; IOP: Intraocular pressure; LPS: Lipopolysaccharides; NLRP3: NOD-, LRR- and pyrin domain-containing protein 3; P2X7R: P2X purinoceptor 7; OPL: Outer plexiform layer; RGC: Retinal ganglion cell

Ethics approval and consent to participate: All procedures were performed in strict accordance with the National Research Council's "Guide for the Care and Use of Laboratory Animals" and were approved by the University of Pennsylvania Institutional Animal Care and Use Committee (IACUC) in protocol #803584.

Consent for publication: N/A

Availability of data and material: All data generated or analyzed during this study are included in this published article and its supplementary information files, or is available from the corresponding author on reasonable request.

Competing interests: The authors declare that they have no competing interests. Dr. Mitchell is named in a patent describing the use of P2X7 receptor in glaucoma but there is no conflict of interest.

Funding: This work was supported by grants R01 EY013434 (CHM), R01 EY015537 (CHM), TL1TR001880 (KC), T32EY007035 (KC) and T32NS043126 (AHJ). The funding bodies played no role in the design of the study and collection, analysis, or interpretation of data and in writing the manuscript. made substantial contributions to the conception and design of the work, the acquisition, analysis and interpretation of data, and drafted the work.

Authors' contributions: KEC made substantial contributions to the conception and design of the work, the acquisition, analysis and interpretation of data, and drafted the work; WL made substantial contributions to the conception and design of the work, the acquisition, analysis and interpretation of data, and helped substantially revise the work; AHJ made substantial contributions to acquisition, analysis and interpretation of data, and helped substantially revise the work; FA made substantial contributions to the acquisition, analysis and interpretation of data; AC made substantial contributions to the acquisition, analysis and interpretation of data; HYT made substantial contributions to the acquisition, analysis and interpretation of data; SPC made substantial contributions to the acquisition and analysis of data; PS made substantial contributions to the acquisition and analysis of data; NMG made substantial contributions to the acquisition and interpretation of data; CHM made substantial contributions to the conception and design of the work, analysis and interpretation of data, and drafted the work. All authors have approved the submitted version and agreed both to be personally accountable for the author's own contributions and to ensure that questions related to the accuracy or integrity of any part of the work, are appropriately investigated, resolved, and the resolution documented in the literature.

Acknowledgements: The authors would like to thank Kelly Jordan-Sciutto for use of the Keyence microscope, Chider Chen for use of the Nanodrop, and Marco Tizano for advice on the Cx3CR1$^{+/GFP}$ mice.

Figure Legends

Figure 1. Retinal P2X7R stimulation leads to activated microglia morphology and gene expression. a, b Retinae injected with Saline or 250 µM BzATP indicated that BzATP exposure results in greater Iba1 expression and different morphology. **c, d** Z-projections of retina wholemounts demonstrate increased Iba1 staining in the IPL and RGC layers of the retina with BzATP exposure. **e** Representations of image tracing and conversion to a binary image for analysis. **f.** Sholl analysis indicates reduced branching complexity of microglia exposed to BzATP (n = 41, 46 cells, 3 biological replicates). **g** Summed branch length is reduced in microglia exposed to BzATP. When compared to Saline (**h**), Cell soma size and Iba1 Intensity are elevated in circled area of microglia from retinae exposed to BzATP (**i**). **j** Quantification of Iba1 intensity in selected area (n=60, 55 cells, 3 biological replicates). **k** Observer scoring of images taken from Saline-exposed or BzATP-exposed retinae supports data indicating that Iba1-positive microglia are activated upon exposure to BzATP. Each dot represents the mean value of 6 trained observers (n = 12, 9 images, 3 biological replicates). **l** Expression of classical activation genes *Nos2, Tnfa*, and alternative activation genes *Arg1, Chil3* is elevated in retinae exposed to BzATP**.** Statistical significance shown at *p<0.05, **p<0.01, ****p<0.0001. Scale bars represent 40 µm (**a**), 15 µm (**d**), 25 µm (**e, f**).

Figure 2. *Ex vivo* retinal wholemount P2X7R stimulation activates microglia. Retinal whole mounts isolated from Cx3CR1-GFP mice revealed increased fluorescence at the optic nerve head compared to control media (**a**) after exposure to 200 µM BzATP for 2 hours (**b**). This elevation in fluorescence was also seen in the Middle Nasal areas when compared to control media (**c**) or after exposure to BzATP (**c**). **d, e** Z-projection of Middle-Nasal retinae exposed to control media or BzATP. Scale bar represents 50 µm.

Figure 3. Isolated microglia express functional P2X7 receptor. **a** Immunocytochemistry indicating absence of GFAP or synaptohysin in primary cultures of retinal microglial cells. **b** qPCR results from cultured retinal microglial cells exposed for 4 hrs to DMSO (Ctrl), 10 ng/ml LPS (LPS), or 10 ng/ml IL-4 (IL4), with changes in relative expression of mRNA for *Nos2, Tnfa, Il1b, Arg1, and YM1* were consistent with microglial cells polarization. (n=6-9 samples from 2-3 biological replicates). **c** Immunostaining indicated presence of P2X7 receptor in primary retinal microglial cells. **d** Representative trace from a retinal microglia cell loaded with Fura-2 showing an elevation in the cytoplasmic Ca^{2+} levels in response to 1 min BzATP (100 µM). The signal is displayed as the ratio of light excited at 340/380 nm and emitted > 520 nm. The response to BzATP was reduced with exposure to 1µM antagonist A839977 (A83) but restored upon wash out. **e** Quantification of the increase in the ratio of light excited at 340nm vs. 380nm, em >520 nm (referred to as "F 340/380"), indicative of cytoplasmic calcium in cells loaded with Fura-2 (n=3-6 cells/replicate, 3 biological replicates. Statistical significance shown at **p<0.01, ***p<0.001, ****p<0.0001. Scale bar represents 20 µm (**a**), and 10 µm (**c**).

Figure 4. Isolated retinal microglia respond to P2X7 receptor stimulation with activation and retraction a Images taken before and after application of isotonic solution (Control), 250 µM BzATP or 250 µM BzATP + 10 µM A839977 (A83). In cells preincubated with 10 µM A839977, BzATP did not alter cell size much. Similar responses were found in >7 experiments. **b** Elevated expression of classical activation marker *Nos2* and alternative activation marker *Arg1* in cultured retinal microglial cells exposed to 1 mM ATP for 4 hrs (n=9-10 samples, 3 biological replicates). **c** Similar gene expression changes were observed when microglial cells were exposed to 200 µM BzATP for 4 hrs (n=3 tests, 1 biological replicate). **d** Representative images of migration 2-part Boyden chamber kit filter indicated that microglia migrate towards a 1 mM ATP gradient. **e** Microglia were isolated from murine brain and subjected to migration. Correlation between number of Hoechst-stained nuclei per well and fluorescence at 340ex/527em (Pearson's correlation r=0.9396 with p=0.0001). **f** Microglia migration to 1 mM ATP was inhibited with preexposure to 10 µM P2Y12 inhibitor AR-C 69931 (ARC) but not 1 µM P2X7-inhibitor A83 (n=17-20 samples, 4 biological replicates). Statistical significance shown as *p<0.05, **p<0.01, ***p<0.001, ****p<0.0001. Scale bars represent 10 µm (**a**), 50 µm (**d**).

Figure 5. Elevation of IOP releases ATP and activates microglia. a Increase in ATP concentration of vitreous humor 24 hrs after elevation of IOP via the controlled elevation of IOP (CEI) procedure (n=3 biological replicates). **b** Immunohistochemical image showing staining for Iba1 (red) in the central nasal quadrant in a retinal whole mount from an unstimulated C57Bl/6J mouse eye. **c** Iba1 staining from an analogous region of an eye after elevation of IOP, and sacrificed 24hrs later.

Retinal microglia subject to IOP elevation showed increased soma size, increased staining for Iba1, and shorter, thicker projections. **d** Quantification of morphological activation of microglia across central and middle regions (n=48, 47 images, 3 biological replicates). **e** Weekly IOP measurements from mice injected with magnetic beads or saline control (n=3). **f** IOP integral, expressed as summed mmHg days exposure over baseline IOP, for bead and saline-injected eyes. **g** Immunohistochemical staining of Iba1 of a cryosection of the central region of saline injected eye outlines elongated processes. **h** Iba1 staining of an analogous region of a retina subjected to 7 weeks of elevation of IOP indicates microglial phenotype emblematic of activation. **i** Quantification of a 5 µm area surrounding the soma indicates significant elevation of Iba1 intensity per cell (n=4 retinae, 3 mice). **j** qPCR showing increased expression of *Nos2, Tnfa, Arg1,* and *Chil3*, as was *Lcn2* in the retina 24 hrs after the CEI procedure. Dots represent change in expression from a single mouse, with expression normalized to the average of unpressurized contralateral eyes (n=4-7 mice). Scale bars represent 20 µm (**b**) and 50 µm (**g**). Statistical significance shown as *p<0.05, **p<0.01, ****p<0.0001.

Figure 6. P2X7 receptor is implicated in microglia activation *in vivo*. a Iba1 staining central nasal quadrant retinal whole mount of $P2X7^{-/-}$ mouse under baseline conditions. **b** Immunohistochemical staining of an analogous region 24 hrs after IOP elevation in $P2X7^{-/-}$ mice. **c** Observer scoring of IHC images of microglial morphology across central and middle regions of $P2X7^{-/-}$ mice suggests no differences between baseline (clear) and CEI (red) (n=48 images, 3 mice). **d** Scoring of baseline conditions was greater in retina from $P2X7^{-/-}$ mice (green) than C57Bl6J mice (clear) (n=48 images, 3 mice). **e** 24 hrs after elevation of IOP, microglial activation scores were

greater in C57 mice than P2X7$^{-/-}$ mice (3 Ctrl, 3 P2X7$^{-/-}$ mice). **f** Increase in retinal expression of *Arg1*, *TNFa*, *iNOS, Chil3* and *Lcn2* found 24 hrs after the CEI procedure in P2RX7$^{-/-}$ mice (n=3-6 mice). **g** Relative change in retinal expression of key genes after the CEI procedure in C57Bl/6J mice compared to P2RX7$^{-/-}$ mice. Values represent mean $\Delta\Delta$CT levels for each gene compared to unpressurized control retinae. Scale bar represents 20 µm. Statistical significance shown as *p<0.05, **p<0.01.

Figure 7. P2X7 receptor stimulation releases cytokine IL-1β. a Mouse retinal microglial cells primed with 1 µg/ml LPS for three hours then exposed to an additional 3 mM ATP released a significant quantity of IL-1β protein into the supernatant relative to LPS alone (Control). Preincubation with 1 µM A83 abolished release (n=12 samples, 4 biological replicates). **b** Similar pattern of IL-1β release was measured in primed microglial cells with 1 hr exposure to 200 µM BzATP (n=9 samples, 3 biological replicates). **c** Gene expression of *Il1b* was elevated in cultured mouse retinal microglia after 4 hr exposure to 1 mM ATP. **d** Gene expression of *Il1b* was upregulated in C57B67 and P2X7$^{-/-}$ retinae after elevated IOP, but that upregulation was significantly less in P2X7R$^{-/-}$ retinae (n=6, 5 mice). **e** Rat microglia primed with 500 ng/ml LPS for 3 hours followed by exposure to an additional 3 mM ATP released significantly more IL-1β than cultured rat astrocytes primed with LPS and 5 ng/ml IL-1α, followed by similar exposure to ATP (n=3 samples from cultures obtained from multiple rats combined). Statistical significance shown as *p<0.05, ****p<0.0001.

Figure 8. Ganglion cell death is correlated to P2X7R stimulation and microglial activation. a Representative images show that staining for RGC marker Brn3a is decreased in retina 22 – 24 hrs after IOP elevation following IOP elevation to control C57Bl/6J mice. **b** Decrease in Brn3a staining was not observed in retinae from $P2X7^{-\backslash -}$ after IOP elevation compared to control. **c** Fewer Brn3a-labeled RGCs were counted in retinae from C57Bl/6J eyes exposed to elevated IOP (red) compared to normotensive controls (clear, left). RGC numbers in control (clear, right) and elevated IOP (green) in $P2X7^{-/-}$ mice were unchanged, demonstrating that there is no pressure-dependent loss of RGCs in the $P2X7^{-/-}$ mice. More Brn3a cells were quantified from $P2X7^{-/-}$ eyes subjected to elevated IOP (green) compared to C57 eyes (red) (n= 42-46 images, 3 mice). **d** Retinal whole mount from a C57Bl/6J mouse showing the spatial relationship between RGCs stained with Brn3a (red) and Iba1 stained microglial (green); images show staining across the central region with the optic nerve head (left) the middle region (center) and peripheral region (right) of the optic disk are shown. **e** Correlation between the loss of RGCs and rise in microglial activation accompanying IOP elevation. (Pearson's correlation with p=0.038; n=7 sections from central and middle regions of 3 control and contralateral CEI retina). **f** No such correlation between RGC loss and microglial activation exists in regions from $P2X7^{-\backslash -}$ mice. Statistical significance show as *p<0.05, ****p<0.0001.

Supplementary Figures

Supplementary Figure S1. List of qPCR primers.

Supplementary Figure S2. a Microglial cell tracing length was quantified and total branch length was normalized to the average summed branch length within each mouse. Total summed branch length was reduced by approximately 10% (Mean saline = 0.9941, mean BzATP = 0.8930). *p<0.05.

Supplementary Figure S3. a Images derived from IBA1-immunostained retinal wholemounts that were evaluated for morphologic or molecular markers of activation and receiving a score of 1, 2, or 3. Scale bar represents 50 µm. **b** Significant correlation between observer scoring and microglial IBA1-soma intensity was found. Each dot represents the mean value among 6 masked, trained observers (n=21 images, 6 retinae).

Supplementary Figure S4. Videos demonstrating microglial retraction with exposure to BzATP. 15 minute videos were recorded at 15 frames per section, with experimental solution added at t = 3 min. **a** Addition of fresh Mg^{2+}-free solution added at 3 minutes led to little or no morphological changes. **b** Addition of 250 µM BzATP at 3 minutes resulted in rapid retraction of microglial extensions and rounding of cells. **c** with preexposure to 10 µM A839977, the addition of 10 µM A839977 + 250 µM BzATP at 3 minutes revealed little reduction in microglia processes.

Supplementary Figure S5. a RGCs and **b** microglia cell numbers were counted per image and averaged within superior inferior, nasal, or temporal regions. There was a significant difference in distribution of RGCs in peripheral retinal areas, where as RGC populations in the central and

middle areas demonstrated homogeneity (n = 12 areas, 3 mice, 2-Way ANOVA with Repeated Measures). ** $p<0.01$, ***$p<0.001$.

References

1. Lawson LJ PV, Dri P, Gordon S: **Heterogeneity in the distribution and morphology of microglia in the normal adult mouse brain.** *Neuroscience* 1990, **39:**151-170.

2. Colonna M BO: **Microglia Function in the Central Nervous System During Health and Neurodegeneration.** *Annu Rev Immunol* 2017, **35:**441-468.

3. Salter MW, Stevens B: **Microglia emerge as central players in brain disease.** *Nat Med* 2017, **23:**1018-1027.

4. Butovsky O, Jedrychowski MP, Cialic R, Krasemann S, Murugaiyan G, Fanek Z, Greco DJ, Wu PM, Doykan CE, Kiner O, et al: **Targeting miR-155 restores abnormal microglia and attenuates disease in SOD1 mice.** *Ann Neurol* 2015, **77:**75-99.

5. Mathys H, Adaikkan C, Gao F, Young JZ, Manet E, Hemberg M, De Jager PL, Ransohoff RM, Regev A, Tsai LH: **Temporal Tracking of Microglia Activation in Neurodegeneration at Single-Cell Resolution.** *Cell Rep* 2017, **21:**366-380.

6. Bosco A, Steele MR, Vetter ML: **Early microglia activation in a mouse model of chronic glaucoma.** *J Comp Neurol* 2011, **519:**599-620.

7. Ito D TK, Suzuki S, Dembo T, Fukuuchi Y: **Enhanced expression of Iba1, ionized calcium-binding adapter molecule 1, after transient focal cerebral ischemia in rat brain.** *Stroke* 2001, **32:**1208-1215.

8. Gonzalez-Prieto M, Gutierrez IL, Garcia-Bueno B, Caso JR, Leza JC, Ortega-Hernandez A, Gomez-Garre D, Madrigal JLM: **Microglial CX3CR1 production increases in Alzheimer's disease and is regulated by noradrenaline.** *Glia* 2021, **69:**73-90.

9. Chen S LD, Streit WJ, Harrison JK: **TGF-beta1 upregulates CX3CR1 expression and inhibits fractalkine-stimulated signaling in rat microglia.** *J Neuroimmunol* 2002, **133:**46-55.

10. Szepesi Z, Manouchehrian O, Bachiller S, Deierborg T: **Bidirectional Microglia-Neuron Communication in Health and Disease.** *Front Cell Neurosci* 2018, **12:**323.

11. Chhor V, Le Charpentier T, Lebon S, Ore MV, Celador IL, Josserand J, Degos V, Jacotot E, Hagberg H, Savman K, et al: **Characterization of phenotype markers and neuronotoxic potential of polarised primary microglia in vitro.** *Brain Behav Immun* 2013, **32:**70-85.

12. Guzman-Martinez L, Maccioni RB, Andrade V, Navarrete LP, Pastor MG, Ramos-Escobar N: **Neuroinflammation as a Common Feature of Neurodegenerative Disorders.** *Front Pharmacol* 2019, **10:**1008.

13. Wooff Y, Man SM, Aggio-Bruce R, Natoli R, Fernando N: **IL-1 Family Members Mediate Cell Death, Inflammation and Angiogenesis in Retinal Degenerative Diseases.** *Front Immunol* 2019, **10:**1618.

14. Liu X, Liu J, Zhao S, Zhang H, Cai W, Cai M, Ji X, Leak RK, Gao Y, Chen J, Hu X: **Interleukin-4 Is Essential for Microglia/Macrophage M2 Polarization and Long-Term Recovery After Cerebral Ischemia.** *Stroke* 2016, **47:**498-504.

15. Jin Q, Cheng J, Liu Y, Wu J, Wang X, Wei S, Zhou X, Qin Z, Jia J, Zhen X: **Improvement of functional recovery by chronic metformin treatment is associated with enhanced alternative activation of microglia/macrophages and increased angiogenesis and neurogenesis following experimental stroke.** *Brain Behav Immun* 2014, **40:**131-142.

16. Kobashi S, Terashima T, Katagi M, Nakae Y, Okano J, Suzuki Y, Urushitani M, Kojima H: **Transplantation of M2-Deviated Microglia Promotes Recovery of Motor Function after Spinal Cord Injury in Mice.** *Mol Ther* 2020, **28:**254-265.

17. Galloway DA, Blandford SN, Berry T, Williams JB, Stefanelli M, Ploughman M, Moore CS: **miR-223 promotes regenerative myeloid cell phenotype and function in the demyelinated central nervous system.** *Glia* 2019, **67:**857-869.

18. Boche D, Perry VH, Nicoll JA: **Review: activation patterns of microglia and their identification in the human brain.** *Neuropathol Appl Neurobiol* 2013, **39:**3-18.

19. Butovsky O, Weiner HL: **Microglial signatures and their role in health and disease.** *Nat Rev Neurosci* 2018, **19:**622-635.

20. Nimmerjahn A, Kirchhoff, F. & Helmchen, F: **Resting microglial cells are highly dynamic surveillants of brain parenchyma in vivo.** *Science* 2005, **308:**1314-1318.

21. Marinelli S, Basilico B, Marrone MC, Ragozzino D: **Microglia-neuron crosstalk: Signaling mechanism and control of synaptic transmission.** *Semin Cell Dev Biol* 2019, **94:**138-151.

22. Olah M BK, Vinet J, Boddeke HWGM: **Microglia Phenotype Diversity.** *Cns Neurological Disord - Drug Targets* 2011, **10:**108-118.

23. Morrison H, Young K, Qureshi M, Rowe RK, Lifshitz J: **Quantitative microglia analyses reveal diverse morphologic responses in the rat cortex after diffuse brain injury.** *Sci Rep* 2017, **7:**13211.

24. Morrison HW FJ: **A quantitative spatiotemporal analysis of microglia morphology during ischemic stroke and reperfusion.** *J Neuroinflammation* 2013, **10:**4.

25. Davis BM, Salinas-Navarro M, Cordeiro MF, Moons L, De Groef L: **Characterizing microglia activation: a spatial statistics approach to maximize information extraction.** *Sci Rep* 2017, **7:**1576.

26. Wyatt-Johnson SK, Herr SA, Brewster AL: **Status Epilepticus Triggers Time-Dependent Alterations in Microglia Abundance and Morphological Phenotypes in the Hippocampus.** *Front Neurol* 2017, **8:**700.

27. Avignone E, Lepleux M, Angibaud J, Nagerl UV: **Altered morphological dynamics of activated microglia after induction of status epilepticus.** *J Neuroinflammation* 2015, **12:**202.

28. Bosco A, Romero CO, Breen KT, Chagovetz AA, Steele MR, Ambati BK, Vetter ML: **Neurodegeneration severity can be predicted from early microglia alterations monitored in vivo in a mouse model of chronic glaucoma.** *Dis Model Mech* 2015, **8:**443-455.

29. Beynon SB, Walker FR: **Microglial activation in the injured and healthy brain: what are we really talking about? Practical and theoretical issues associated with the measurement of changes in microglial morphology.** *Neuroscience* 2012, **225:**162-171.

30. Yuan L NA: **Activated microglia in the human glaucomatous optic nerve head.** *J Neurosci Res* 2001, **64:**523-532.

31. Li A, Zhang X, Zheng D, Ge J, Laties AM, Mitchell CH: **Sustained elevation of extracellular ATP in aqueous humor from humans with primary chronic angle-closure glaucoma.** *Exp Eye Res* 2011, **93:**528-533

32. Lu W, Hu H, Sevigny J, Gabelt BT, Kaufman PL, Johnson EC, Morrison JC, Zode GS, Sheffield VC, Zhang X, et al: **Rat, mouse, and primate models of chronic glaucoma show sustained elevation of extracellular ATP and altered purinergic signaling in the posterior eye.** *Invest Ophthalmol Vis Sci* 2015, **56:**3075-3083.

33. Reigada D, Lu W, Zhang M, Mitchell CH: **Elevated pressure triggers a physiological release of ATP from the retina: Possible role for pannexin hemichannels.** *Neuroscience* 2008, **157:**396-404

34. Sadananda P, Shang F, Liu L, Mansfield KJ, Burcher E: **Release of ATP from rat urinary bladder mucosa: role of acid, vanilloids and stretch.** *Br J Pharmacol* 2009, **158:**1655-1662.

35. Takahara N, Ito S, Furuya K, Naruse K, Aso H, Kondo M, Sokabe M, Hasegawa Y: **Real-time imaging of ATP release induced by mechanical stretch in human airway smooth muscle cells.** *Am J Respir Cell Mol Biol* 2014, **51:**772-782.

36. Wei L, Mousawi F, Li D, Roger S, Li J, Yang X, Jiang LH: **Adenosine Triphosphate Release and P2 Receptor Signaling in Piezo1 Channel-Dependent Mechanoregulation.** *Front Pharmacol* 2019, **10:**1304.

37. Beckel JM, Gomez NM, Lu W, Campagno KE, Nabet B, Albalawi F, Lim JC, Boesze-Battaglia K, Mitchell CH: **Stimulation of TLR3 triggers release of lysosomal ATP in astrocytes and epithelial cells that requires TRPML1 channels.** *Sci Rep* 2018, **8:**5726. .

38. Imura Y, Morizawa Y, Komatsu R, Shibata K, Shinozaki Y, Kasai H, Moriishi K, Moriyama Y, Koizumi S: **Microglia release ATP by exocytosis.** *Glia* 2013, **61:**1320-1330.

39. Coddou C, Yan Z, Obsil T, Huidobro-Toro JP, Stojilkovic SS: **Activation and regulation of purinergic P2X receptor channels.** *Pharmacol Rev* 2011, **63:**641-683.

40. Kaczmarek-Hajek K, Zhang J, Kopp R, Grosche A, Rissiek B, Saul A, Bruzzone S, Engel T, Jooss T, Krautloher A, et al: **Re-evaluation of neuronal P2X7 expression using novel mouse models and a P2X7-specific nanobody.** *Elife* 2018, **7**.

41. Adinolfi E, Giuliani AL, De Marchi E, Pegoraro A, Orioli E, Di Virgilio F: **The P2X7 receptor: A main player in inflammation.** *Biochem Pharmacol* 2018, **151:**234-244.

42. Kopp R, Krautloher A, Ramirez-Fernandez A, Nicke A: **P2X7 Interactions and Signaling - Making Head or Tail of It.** *Front Mol Neurosci* 2019, **12:**183.

43. Orioli E, De Marchi E, Giuliani AL, Adinolfi E: **P2X7 Receptor Orchestrates Multiple Signalling Pathways Triggering Inflammation, Autophagy and Metabolic/Trophic Responses.** *Curr Med Chem* 2017, **24:**2261-2275.

44. Campagno KE, Mitchell CH: **The P2X7 Receptor in Microglial Cells Modulates the Endolysosomal Axis, Autophagy, and Phagocytosis.** *Frontiers in Cellular Neuroscience* 2021, **15**.

45. Aires ID, Boia R, Rodrigues-Neves AC, Madeira MH, Marques C, Ambrosio AF, Santiago AR: **Blockade of microglial adenosine A2A receptor suppresses elevated pressure-induced inflammation, oxidative stress, and cell death in retinal cells.** *Glia* 2019, **67:**896-914.

46. Mitchell CH, Lu W, Hu H, Zhang X, Reigada D, Zhang M: **The P2X(7) receptor in retinal ganglion cells: A neuronal model of pressure-induced damage and protection by a shifting purinergic balance.** *Purinergic Signal* 2009, **5:**241-249

47. Dong L, Hu Y, Zhou L, Cheng X: **P2X7 receptor antagonist protects retinal ganglion cells by inhibiting microglial activation in a rat chronic ocular hypertension model.** *Mol Med Rep* 2018, **17:**2289-2296.

48. Sugiyama T, Lee SY, Horie T, Oku H, Takai S, Tanioka H, Kuriki Y, Kojima S, Ikeda T: **P2X7 receptor activation may be involved in neuronal loss in the retinal ganglion cell layer after acute elevation of intraocular pressure in rats.** *Molecular Vision* 2013, **19:**2080-2091.

49. He Y, Taylor N, Fourgeaud L, Bhattacharya A: **The role of microglial P2X7: modulation of cell death and cytokine release.** *J Neuroinflammation* 2017, **14:**135.

50. Hu H, Lu W, Zhang M, Zhang X, Argall AJ, Patel S, Lee GE, Kim YC, Jacobson KA, Laties AM, Mitchell CH: **Stimulation of the P2X7 receptor kills rat retinal ganglion cells in vivo.** *Exp Eye Res* 2010, **91:**425-432

51. Schindelin J, Arganda-Carreras I, Frise E, Kaynig V, Longair M, Pietzsch T, Preibisch S, Rueden C, Saalfeld S, Schmid B, et al: **Fiji: an open-source platform for biological-image analysis.** *Nat Methods* 2012, **9:**676-682.

52. Longair MH, Baker DA, Armstrong JD: **Simple Neurite Tracer: open source software for reconstruction, visualization and analysis of neuronal processes.** *Bioinformatics* 2011, **27:**2453-2454.

53. Lu W, Albalawi F, Beckel JM, Lim JC, Laties AM, Mitchell CH: **The P2X7 receptor links mechanical strain to cytokine IL-6 up-regulation and release in neurons and astrocytes.** *J Neurochem* 2017, **141:**436-448.

54. Roque RS CR: **Isolation and culture of retinal microglia.** *Curr Eye Res* 1993, **12:**285-290.

55. Ma W, Zhao L, Fontainhas AM, Fariss RN, Wong WT: **Microglia in the mouse retina alter the structure and function of retinal pigmented epithelial cells: a potential cellular interaction relevant to AMD.** *PLoS One* 2009, **4:**e7945.

56. Lian H, Roy E, Zheng H: **Protocol for Primary Microglial Culture Preparation.** *Bio Protoc* 2016, **6**.

57. Collins HY, Bohlen CJ: **Isolation and Culture of Rodent Microglia to Promote a Dynamic Ramified Morphology in Serum-free Medium.** *J Vis Exp* 2018.

58. Lim JC, Lu W, Beckel JM, Mitchell CH: **Neuronal release of cytokine IL-3 triggered by mechanosensitive autostimulation of the P2X7 receptor Is neuroprotective.** *Front Cell Neurosci* 2016, **10:**270.

59. Gómez NM, Lu W, Lim J, Kiselyov K, Grishchuk Y, Slaugenhaupt S, Pfeffer B, Fliesler SJ, CH. M: **Robust lysosomal calcium signaling through channel TRPML1 is impaired by lipofuscin accumulation** *Faseb J* 2018, **32:**782-794

60. Tehrani S, Davis L, Cepurna WO, Choe TE, Lozano DC, Monfared A, Cooper L, Cheng J, Johnson EC, Morrison JC: **Astrocyte Structural and Molecular Response to Elevated Intraocular Pressure Occurs Rapidly and Precedes Axonal Tubulin Rearrangement within the Optic Nerve Head in a Rat Model.** *PLoS One* 2016, **11:**e0167364.

61. Crowston JG, Kong YX, Trounce IA, Dang TM, Fahy ET, Bui BV, Morrison JC, Chrysostomou V: **An acute intraocular pressure challenge to assess retinal ganglion cell injury and recovery in the mouse.** *Exp Eye Res* 2015, **141:**3-8.

62. Albalawi F, Lu W, Beckel JM, Lim JC, McCaughey SA, Mitchell CH: **The P2X7 Receptor Primes IL-1beta and the NLRP3 Inflammasome in Astrocytes Exposed to Mechanical Strain.** *Front Cell Neurosci* 2017, **11:**227.

63. Jassim AH, Inman DM: **Evidence of Hypoxic Glial Cells in a Model of Ocular Hypertension.** *Invest Ophthalmol Vis Sci* 2019, **60:**1-15.

64. Samsel PA, Kisiswa L, Erichsen JT, Cross SD, Morgan JE: **A novel method for the induction of experimental glaucoma using magnetic microspheres.** *Invest Ophthalmol Vis Sci* 2011, **52:**1671-1675.

65. Rojas B GB, Ramírez AI, Salazar JJ, de Hoz R, Valiente-Soriano FJ, Avilés-Trigueros M, Villegas-Perez MP, Vidal-Sanz M, Triviño A, Ramírez JM: **Microglia in mouse retina contralateral to experimental glaucoma exhibit multiple signs of activation in all retinal layers.** *J Neuroinflammation* 2014, **11**.

66. Silverman SM WW: **Microglia in the Retina: Roles in Development, Maturity, and Disease.** *Annu Rev Vis Sci* 2018, **4:**45-77.

67. O'Koren EG, Yu C, Klingeborn M, Wong AYW, Prigge CL, Mathew R, Kalnitsky J, Msallam RA, Silvin A, Kay JN, et al: **Microglial Function Is Distinct in Different Anatomical Locations during Retinal Homeostasis and Degeneration.** *Immunity* 2019, **50:**723-737 e727.

68. Akhmetzyanova E, Kletenkov K, Mukhamedshina Y, Rizvanov A: **Different Approaches to Modulation of Microglia Phenotypes After Spinal Cord Injury.** *Front Syst Neurosci* 2019, **13:**37.

69. Hu X, Leak RK, Shi Y, Suenaga J, Gao Y, Zheng P, Chen J: **Microglial and macrophage polarization-new prospects for brain repair.** *Nat Rev Neurol* 2015, **11:**56-64.

70. Liu X, Wen S, Yan F, Liu K, Liu L, Wang L, Zhao S, Ji X: **Salidroside provides neuroprotection by modulating microglial polarization after cerebral ischemia.** *J Neuroinflammation* 2018, **15:**39.

71. Wes PD, Holtman IR, Boddeke EW, Moller T, Eggen BJ: **Next generation transcriptomics and genomics elucidate biological complexity of microglia in health and disease.** *Glia* 2016, **64:**197-213.

72. Cherry JD, Olschowka JA, O'Banion MK: **Arginase 1+ microglia reduce Abeta plaque deposition during IL-1beta-dependent neuroinflammation.** *J Neuroinflammation* 2015, **12:**203.

73. Ransohoff RM: **A polarizing question: do M1 and M2 microglia exist?** *Nat Neurosci* 2016, **19:**987-991.

74. Bronstein R, Torres L, Nissen JC, Tsirka SE: **Culturing microglia from the neonatal and adult central nervous system.** *J Vis Exp* 2013**:**50647.

75. Lively S, Schlichter LC: **Microglia Responses to Pro-inflammatory Stimuli (LPS, IFNgamma+TNFalpha) and Reprogramming by Resolving Cytokines (IL-4, IL-10).** *Front Cell Neurosci* 2018, **12:**215.

76. Guha S, Baltazar GC, Coffey EE, Tu L-A, Lim JC, Beckel JM, Eysteinsson T, Lu W, O'Brien-Jenkins A, Patel S, et al: **Lysosomal alkalinization, lipid oxidation, impaired autophagy and reduced phagosome clearance triggered by P2X7 receptor activation in retinal pigmented epithelial cells** *Faseb J* 2013, **27** 4500-4509.

77. Honore P, Donnelly-Roberts D, Namovic M, Zhong C, Wade C, Chandran P, Zhu C, Carroll W, Perez-Medrano A, Iwakura Y, Jarvis MF: **The antihyperalgesic activity of a selective**

P2X7 receptor antagonist, A-839977, is lost in IL-1alphabeta knockout mice. *Behav Brain Res* 2009, **204:**77-81.

78. Lee S, Lee J, Kim S, Park JY, Lee WH, Mori K, Kim SH, Kim IK, Suk K: **A dual role of lipocalin 2 in the apoptosis and deramification of activated microglia.** *J Immunol* 2007, **179:**3231-3241.

79. Parmar T, Parmar VM, Perusek L, Georges A, Takahashi M, Crabb JW, Maeda A: **Lipocalin 2 Plays an Important Role in Regulating Inflammation in Retinal Degeneration.** *J Immunol* 2018, **200:**3128-3141.

80. Feng J, Xu J: **Identification of pathogenic genes and transcription factors in glaucoma.** *Mol Med Rep* 2019, **20:**216-224.

81. Chun BY, Kim JH, Nam Y, Huh MI, Han S, Suk K: **Pathological Involvement of Astrocyte-Derived Lipocalin-2 in the Demyelinating Optic Neuritis.** *Invest Ophthalmol Vis Sci* 2015, **56:**3691-3698.

82. Naskar R WM, Thanos S: **Detection of early neuron degeneration and accompanying microglial responses in the retina of a rat model of glaucoma.** *Invest Ophthalmol Vis Sci* 2002, **43:**2962-2968.

83. Collo G NS, Kawashima E, Kosco-Vilbois M, North RA, Buell G: **Tissue distribution of the P2X7 receptor.** *Neuropharmacology* 1997, **36:**1277-1283.

84. Donnelly-Roberts DL, Namovic MT, Han P, Jarvis MF: **Mammalian P2X7 receptor pharmacology: comparison of recombinant mouse, rat and human P2X7 receptors.** *British journal of pharmacology* 2009, **157:**1203-1214.

85. Young MT, Pelegrin P, Surprenant A: **Amino acid residues in the P2X7 receptor that mediate differential sensitivity to ATP and BzATP.** *Mol Pharmacol* 2007, **71:**92-100.

86. Donnelly-Roberts DL, Namovic MT, Han P, Jarvis MF: **Mammalian P2X7 receptor pharmacology: comparison of recombinant mouse, rat and human P2X7 receptors.** *Br J Pharmacol* 2009, **157:**1203-1214.

87. Di Virgilio F: **P2X7 is a cytotoxic receptor....maybe not: implications for cancer.** *Purinergic Signal* 2020.

88. Burnstock G, Knight GE: **The potential of P2X7 receptors as a therapeutic target, including inflammation and tumour progression.** *Purinergic Signal* 2018, **14:**1-18.

89. Sperlagh B, Illes P: **P2X7 receptor: an emerging target in central nervous system diseases.** *Trends Pharmacol Sci* 2014, **35:**537-547.

90. Fabbrizio P, Amadio S, Apolloni S, Volonte C: **P2X7 Receptor Activation Modulates Autophagy in SOD1-G93A Mouse Microglia.** *Front Cell Neurosci* 2017, **11:**249.

91. Morganti JM, Riparip LK, Rosi S: **Call Off the Dog(ma): M1/M2 Polarization Is Concurrent following Traumatic Brain Injury.** *PLoS One* 2016, **11:**e0148001.

92. Bryant CE SD, Gangloff M, Gay NJ: **The molecular basis of the host response to lipopolysaccharide.** *Nat Rev Microbiol* 2010, **8:**8-14.

93. Zhao R, Ying M, Gu S, Yin W, Li Y, Yuan H, Fang S, Li M: **Cysteinyl Leukotriene Receptor 2 is Involved in Inflammation and Neuronal Damage by Mediating Microglia M1/M2 Polarization through NF-kappaB Pathway.** *Neuroscience* 2019, **422:**99-118.

94. Zhao Q, Wu X, Yan S, Xie X, Fan Y, Zhang J, Peng C, You Z: **The antidepressant-like effects of pioglitazone in a chronic mild stress mouse model are associated with PPARgamma-**

mediated alteration of microglial activation phenotypes. *J Neuroinflammation* 2016, **13:**259.

95. Liu Y, Xiao Y, Li Z: **P2X7 receptor positively regulates MyD88-dependent NF-kappaB activation.** *Cytokine* 2011, **55:**229-236.

96. Chen S, Ye J, Chen X, Shi J, Wu W, Lin W, Lin W, Li Y, Fu H, Li S: **Valproic acid attenuates traumatic spinal cord injury-induced inflammation via STAT1 and NF-kappaB pathway dependent of HDAC3.** *J Neuroinflammation* 2018, **15:**150.

97. Mackenzie AB, Young MT, Adinolfi E, Surprenant A: **Pseudoapoptosis induced by brief activation of ATP-gated P2X7 receptors.** *J Biol Chem* 2005, **280:**33968-33976.

98. Burguillos MA, Deierborg T, Kavanagh E, Persson A, Hajji N, Garcia-Quintanilla A, Cano J, Brundin P, Englund E, Venero JL, Joseph B: **Caspase signalling controls microglia activation and neurotoxicity.** *Nature* 2011, **472:**319-324.

99. Kong Q, Wang M, Liao Z, Camden JM, Yu S, Simonyi A, Sun GY, Gonzalez FA, Erb L, Seye CI, Weisman GA: **P2X(7) nucleotide receptors mediate caspase-8/9/3-dependent apoptosis in rat primary cortical neurons.** *Purinergic Signal* 2005, **1:**337-347.

100. Bidula S, Dhuna K, Helliwell R, Stokes L: **Positive allosteric modulation of P2X7 promotes apoptotic cell death over lytic cell death responses in macrophages.** *Cell Death Dis* 2019, **10:**882.

101. Paolicelli RC, Bisht K, Tremblay ME: **Fractalkine regulation of microglial physiology and consequences on the brain and behavior.** *Front Cell Neurosci* 2014, **8:**129.

102. Jung S AJ, Graemmel P, Sunshine MJ, Kreutzberg GW, Sher A, Littman DR: **Analysis of fractalkine receptor CX(3)CR1 function by targeted deletion and green fluorescent protein reporter gene insertion.** *Mol Cell Biol* 2000, **20:**4106-4114.

103. Wang K, Peng B, Lin B: **Fractalkine receptor regulates microglial neurotoxicity in an experimental mouse glaucoma model.** *Glia* 2014, **62:**1943-1954.

104. Zabel MK, Zhao L, Zhang Y, Gonzalez SR, Ma W, Wang X, Fariss RN, Wong WT: **Microglial phagocytosis and activation underlying photoreceptor degeneration is regulated by CX3CL1-CX3CR1 signaling in a mouse model of retinitis pigmentosa.** *Glia* 2016, **64:**1479-1491.

105. Hu SJ, Calippe B, Lavalette S, Roubeix C, Montassar F, Housset M, Levy O, Delarasse C, Paques M, Sahel JA, et al: **Upregulation of P2RX7 in Cx3cr1-Deficient Mononuclear Phagocytes Leads to Increased Interleukin-1beta Secretion and Photoreceptor Neurodegeneration.** *J Neurosci* 2015, **35:**6987-6996.

106. Meuth SG, Simon OJ, Grimm A, Melzer N, Herrmann AM, Spitzer P, Landgraf P, Wiendl H: **CNS inflammation and neuronal degeneration is aggravated by impaired CD200-CD200R-mediated macrophage silencing.** *J Neuroimmunol* 2008, **194:**62-69.

107. Finneran DJ, Nash KR: **Neuroinflammation and fractalkine signaling in Alzheimer's disease.** *J Neuroinflammation* 2019, **16:**30.

108. Zhang X, Zhang M, Laties AM, Mitchell CH: **Stimulation of P2X7 receptors elevates Ca2+ and kills retinal ganglion cells.** *Invest Ophthalmol Vis Sci* 2005, **46:**2183-2191.

109. Rodrigues-Neves AC, Aires ID, Vindeirinho J, Boia R, Madeira MH, Goncalves FQ, Cunha RA, Santos PF, Ambrosio AF, Santiago AR: **Elevated Pressure Changes the Purinergic System of Microglial Cells.** *Front Pharmacol* 2018, **9:**16.

110. Zhang Y, Xu Y, Sun Q, Xue S, Guan H, Ji M: **Activation of P2X7R- NLRP3 pathway in Retinal microglia contribute to Retinal Ganglion Cells death in chronic ocular hypertension (COH).** *Exp Eye Res* 2019, **188:**107771.

111. Bianchi BR LK, Touma E, Niforatos W, Burgard EC, Alexander KM, et al: **Pharmacological characterization of recombinant human and rat P2X receptor subtypes.** *Eur J Pharmacol* 1999, **376:**127-138.

112. Guttenplan KA, Stafford BK, El-Danaf RN, Adler DI, Munch AE, Weigel MK, Huberman AD, Liddelow SA: **Neurotoxic Reactive Astrocytes Drive Neuronal Death after Retinal Injury.** *Cell Rep* 2020, **31:**107776.

113. Liddelow SA, Guttenplan KA, Clarke LE, Bennett FC, Bohlen CJ, Schirmer L, Bennett ML, Munch AE, Chung WS, Peterson TC, et al: **Neurotoxic reactive astrocytes are induced by activated microglia.** *Nature* 2017, **541:**481-487.

114. Sterling JK, Adetunji MO, Guttha S, Bargoud AR, Uyhazi KE, Ross AG, Dunaief JL, Cui QN: **GLP-1 Receptor Agonist NLY01 Reduces Retinal Inflammation and Neuron Death Secondary to Ocular Hypertension.** *Cell Rep* 2020, **33:**108271.

115. Wang AYM, Wong VHY, Lee PY, Bui BV, Dudczig S, Vessey KA, Fletcher EL: **Retinal ganglion cell dysfunction in mice following acute intraocular pressure is exacerbated by P2X7 receptor knockout.** *Sci Rep* 2021, **11:**4184.

116. Ortega F, Perez-Sen R, Delicado EG, Miras-Portugal MT: **P2X7 nucleotide receptor is coupled to GSK-3 inhibition and neuroprotection in cerebellar granule neurons.** *Neurotox Res* 2009, **15:**193-204.

117. Monif M, Reid CA, Powell KL, Drummond KJ, O'Brien TJ, Williams DA: **Interleukin-1beta has trophic effects in microglia and its release is mediated by P2X7R pore.** *J Neuroinflammation* 2016, **13:**173.

118. Todd L, Palazzo I, Suarez L, Liu X, Volkov L, Hoang TV, Campbell WA, Blackshaw S, Quan N, Fischer AJ: **Reactive microglia and IL1beta/IL-1R1-signaling mediate neuroprotection in excitotoxin-damaged mouse retina.** *J Neuroinflammation* 2019, **16:**118.

119. Sato A OH, Tsumuraya T, Song D, Ohara K, Asano M, Iwakura Y, Atsumi T, Shioda S: **Interleukin-1 participates in the classical and alternative activation of microglia/macrophages after spinal cord injury.** *J Neuroinflammation* 2012, **9:**65.

120. Liu J LW, Reigada D, Nguyen J, Laties AM, Mitchell CH: **Restoration of Lysosomal pH in RPE Cells from Cultured Human and ABCA4−/− Mice: Pharmacologic Approaches and Functional Recovery.** *Invest Ophthalmol Vis Sci* 2008, **49:**772-780.

121. Liu X, Nemeth DP, McKim DB, Zhu L, DiSabato DJ, Berdysz O, Gorantla G, Oliver B, Witcher KG, Wang Y, et al: **Cell-Type-Specific Interleukin 1 Receptor 1 Signaling in the Brain Regulates Distinct Neuroimmune Activities.** *Immunity* 2019, **50:**317-333 e316.

122. Fletcher EL, Wang AY, Jobling AI, Rutar MV, Greferath U, Gu B, Vessey KA: **Targeting P2X7 receptors as a means for treating retinal disease.** *Drug Discov Today* 2019, **24:**1598-1605.

Figure 1

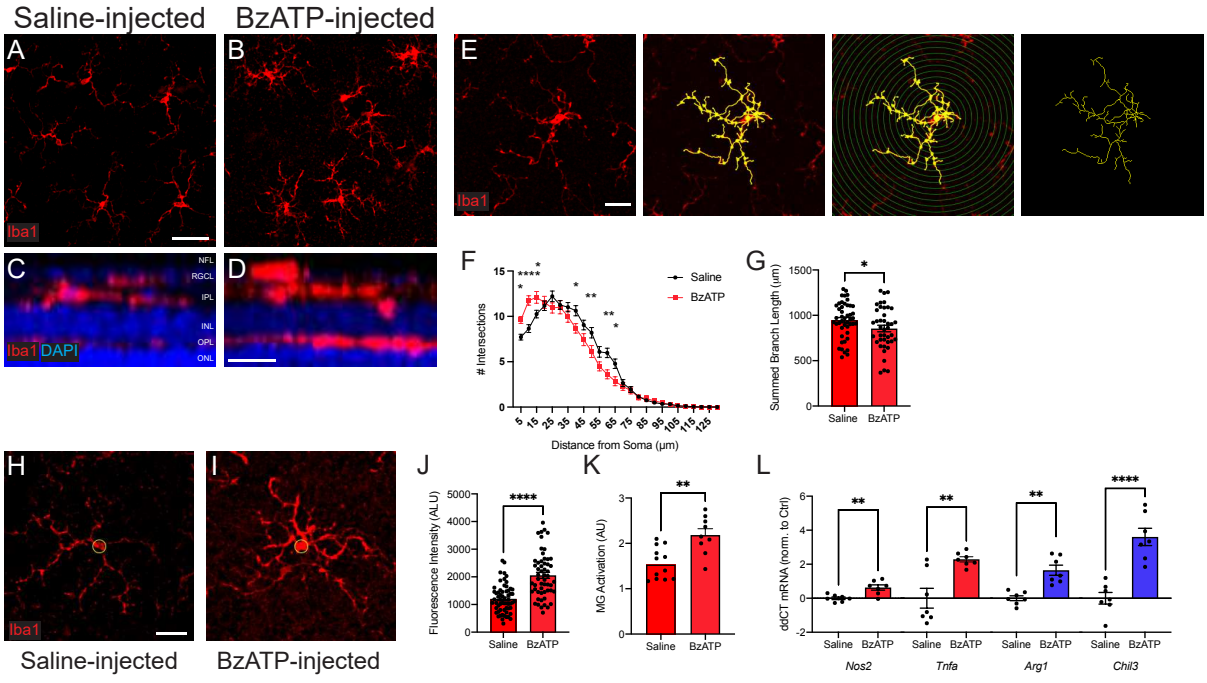
Saline-injected
BzATP-injected
A
B
Iba1
C
D
NFL
RGCL
IPL
INL
OPL
ONL
Iba1 DAPI
E
Iba1
F
Intersections
Distance from Soma (µm)
Saline
BzATP
G
Summed Branch Length (µm)
H
I
Iba1
Saline-injected
BzATP-injected
J
Fluorescence Intensity (A.U)
K
MG Activation (AU)
L
ddCT mRNA (norm. to Ctrl)
Nos2
Tnfa
Arg1
Chil3

Figure 2

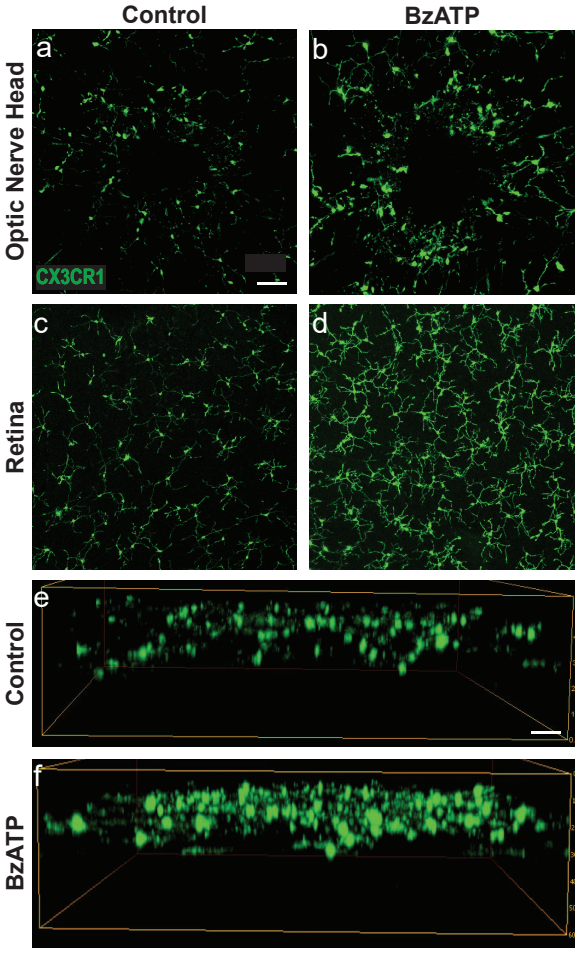
Control
BzATP
Optic Nerve Head
Retina
Control
BzATP
a
b
c
d
e
f
CX3CR1

Figure 3

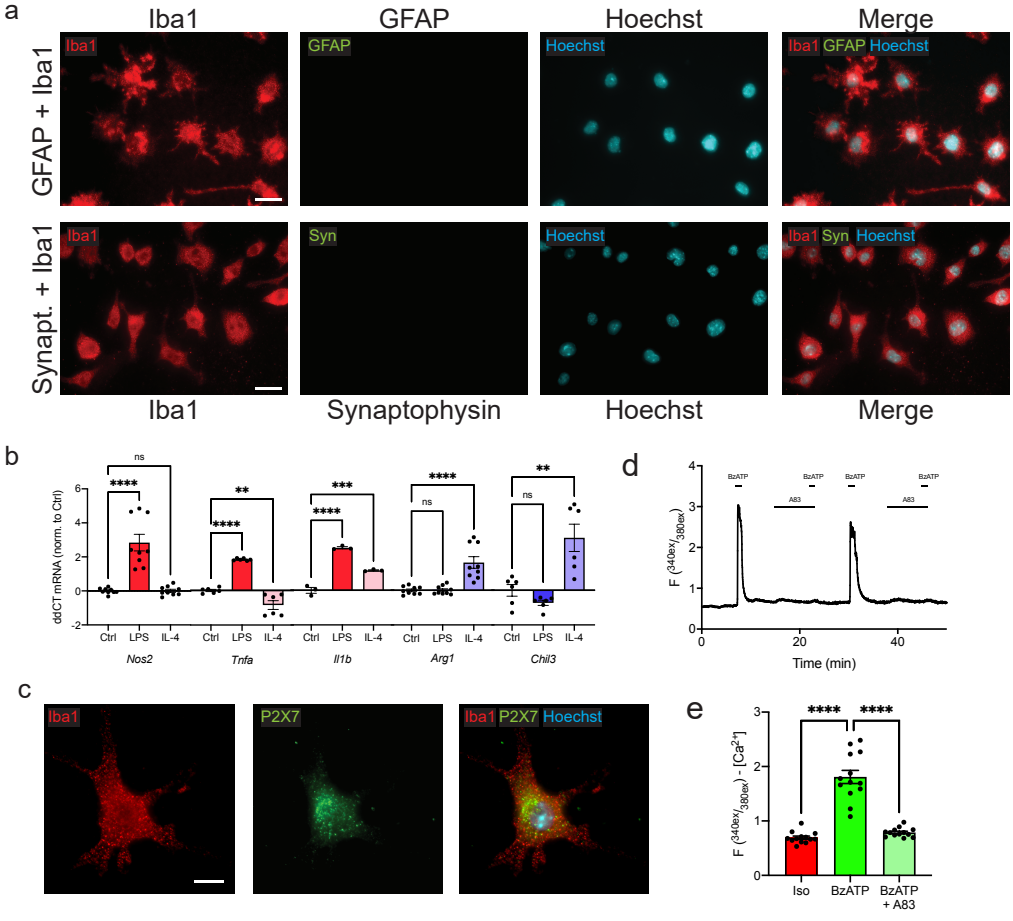
a
Iba1
GFAP
Hoechst
Merge
GFAP + Iba1
Synapt. + Iba1
Iba1
Synaptophysin
Hoechst
Merge
b
ddCT mRNA (norm. to Ctrl)
Ctrl
LPS
IL-4
Nos2
Tnfa
Il1b
Arg1
Chil3
c
Iba1
P2X7
Hoechst
d
BzATP
A83
F (340ex/380ex)
Time (min)
e
F (340ex/380ex) - [Ca2+]
Iso
BzATP
BzATP + A83

Figure 4

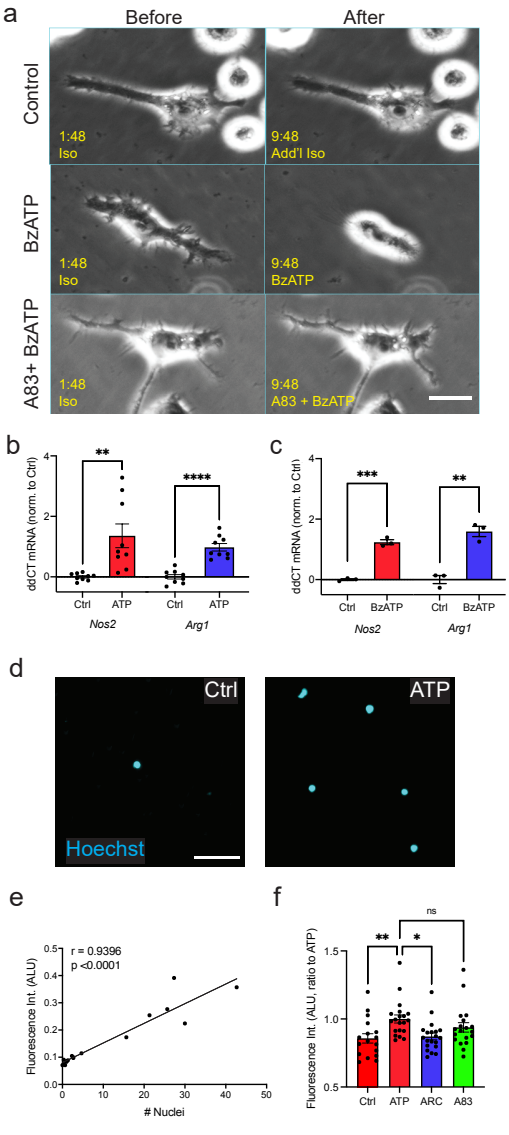
a
Before
After
Control
BzATP
A83+ BzATP
1:48
Iso
9:48
Add'l Iso
1:48
Iso
9:48
BzATP
1:48
Iso
9:48
A83 + BzATP
b
ddCT mRNA (norm. to Ctrl)
**
****
Ctrl
ATP
Ctrl
ATP
Nos2
Arg1
c
ddCT mRNA (norm. to Ctrl)
***
**
Ctrl
BzATP
Ctrl
BzATP
Nos2
Arg1
d
Ctrl
ATP
Hoechst
e
r = 0.9396
p <0.0001
Fluorescence Int. (ALU)
Nuclei
f
ns
**
*
Fluorescence Int. (ALU, ratio to ATP)
Ctrl
ATP
ARC
A83

Figure 5

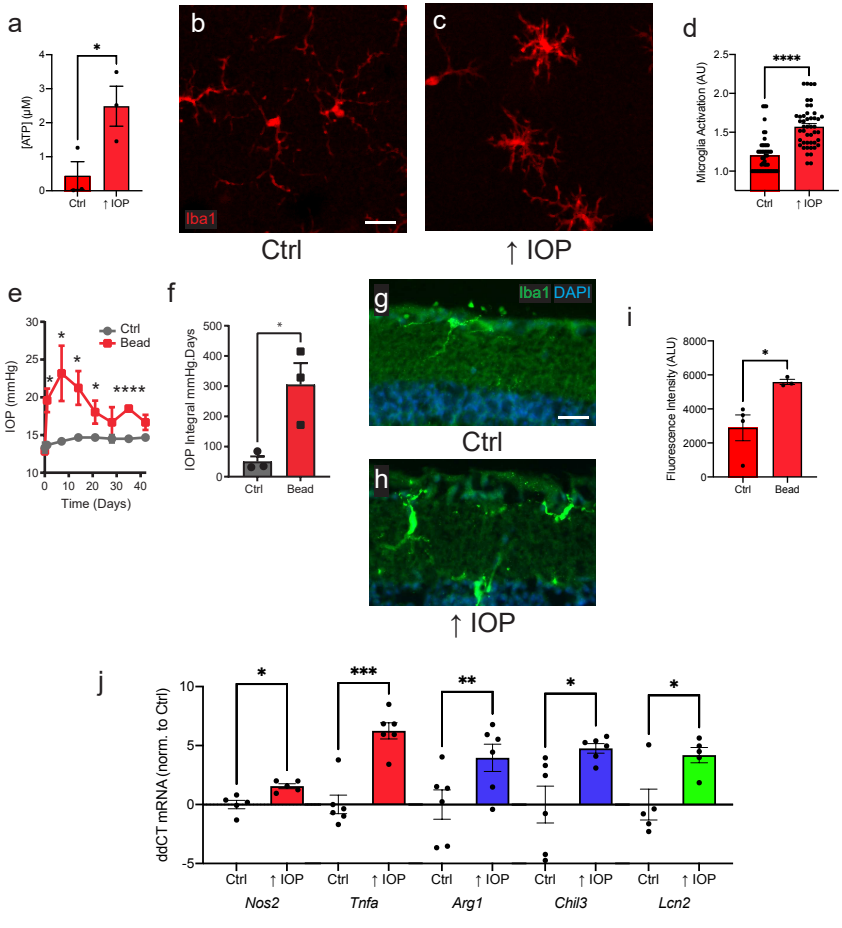
a
[ATP] (μM)
Ctrl
↑ IOP
b
Iba1
c
Ctrl
↑ IOP
d
Microglia Activation (AU)
****
Ctrl
↑ IOP
e
IOP (mmHg)
Ctrl
Bead
Time (Days)
f
IOP Integral mmHg.Days
Ctrl
Bead
g
Iba1 DAPI
Ctrl
h
↑ IOP
i
Fluorescence Intensity (ALU)
Ctrl
Bead
j
ddCT mRNA (norm. to Ctrl)
Ctrl
↑ IOP
Nos2
Tnfa
Arg1
Chil3
Lcn2

Figure 6

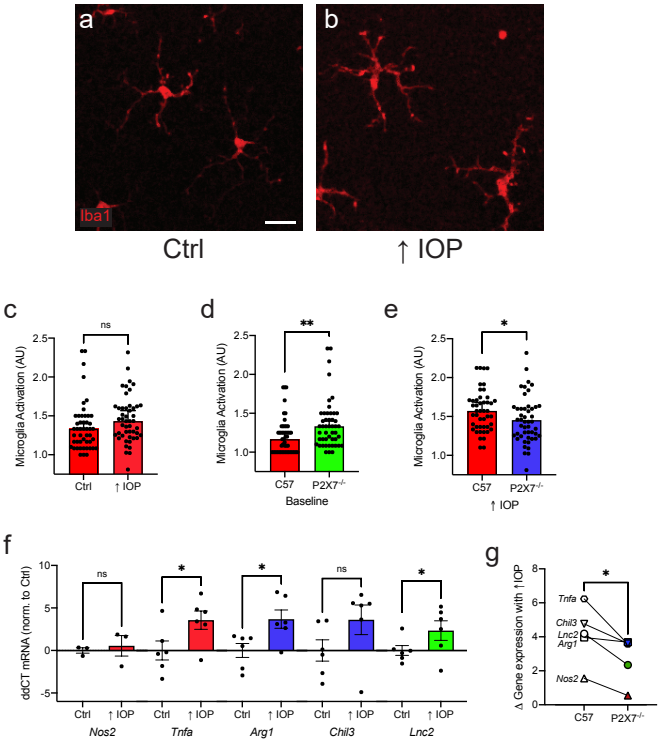
a
b
Iba1
Ctrl
↑ IOP
c
d
e
Microglia Activation (AU)
ns
**
*
Ctrl
↑ IOP
C57
P2X7-/-
Baseline
↑ IOP
f
g
ddCT mRNA (norm. to Ctrl)
Nos2
Tnfa
Arg1
Chil3
Lnc2
Δ Gene expression with ↑IOP
Tnfa
Chil3
Lnc2
Arg1
Nos2

Figure 7

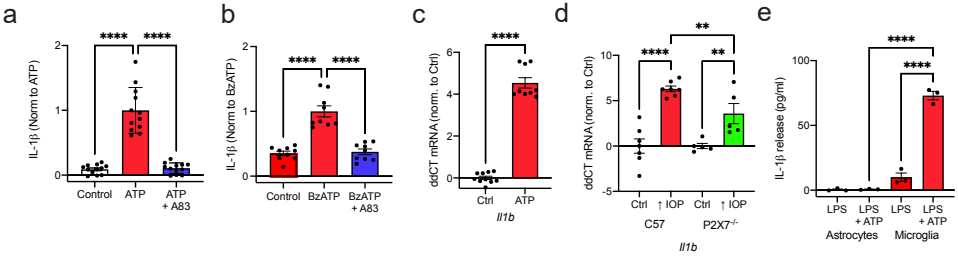
a
IL-1β (Norm to ATP)
****
****
Control
ATP
ATP + A83
b
IL-1β (Norm to BzATP)
****
****
Control
BzATP
BzATP + A83
c
ddCT mRNA (norm. to Ctrl)
****
Ctrl
ATP
Il1b
d
ddCT mRNA (norm. to Ctrl)
**
****
**
Ctrl
↑ IOP
Ctrl
↑ IOP
C57
P2X7-/-
Il1b
e
IL-1β release (pg/ml)
****
****
LPS
LPS + ATP
LPS
LPS + ATP
Astrocytes
Microglia

Figure 8

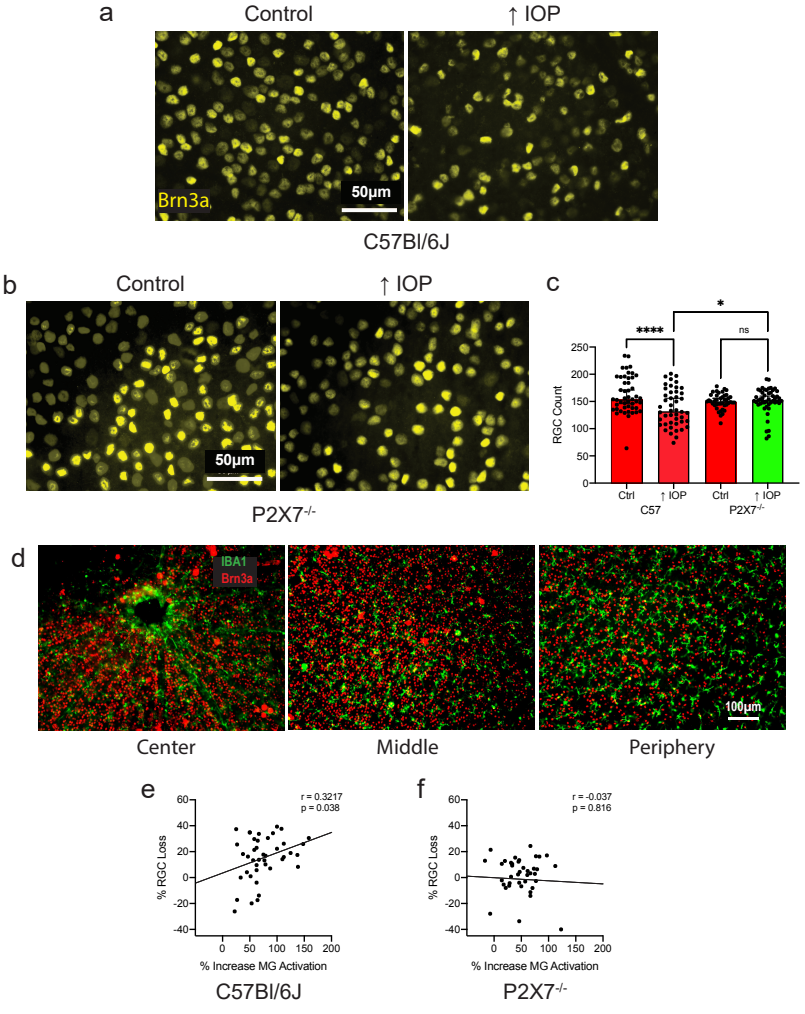
a
Control
↑ IOP
Brn3a
50µm
C57Bl/6J
b
Control
↑ IOP
50µm
P2X7-/-
c
****
*
ns
RGC Count
250
200
150
100
50
0
Ctrl
↑ IOP
Ctrl
↑ IOP
C57
P2X7-/-
d
IBA1
Brn3a
100µm
Center
Middle
Periphery
e
r = 0.3217
p = 0.038
% RGC Loss
60
40
20
0
-20
-40
0
50
100
150
200
% Increase MG Activation
C57Bl/6J
f
r = -0.037
p = 0.816
% RGC Loss
% Increase MG Activation
P2X7-/-

Supplementary figure 1: List of primers used for qPCR

Gene Name	GenBank accession	Forward Primer (5'-3')	Reverse Primer (3'-5')	Size (bp)
Nos2	NM_010927.4	CCCTTCAATGGTTGGTACATGG	ACATTGATCTCCGTGACAGCC	158
Tnfa	NM_013693.3	AAATGGCCTCCCTCTCATCAG	GTCACTCGAATTTTGAGAAGATGATC	73
Arg1	NM_007482.3	ACAAGACAGGGCTCCTTTCAG	GGCTTATGGTTACCCTCCCG	148
Chil3 (cells)	NM_009892.3	AGAAGGGAGTTTCAAACCTGGT	GTCTTGCTCATGTGTGTAAGTGA	109
Chil3 (tissue)	NM_009892.3	GAAGGAGCCACTGAGGTCTG	GAGCCACTGAGCCTTCAAC	114
Lcn2	NM_008491.1	GGAACGTTTCACCCGCTTTG	TGAACCATTGGGTCTCTGCG	140
GAPDH	NM_017008	TCACCACCATGGAGAAGGC	GCTAAGCAGTTGGTGGTGCA	169

Supplemental Figure 2

a

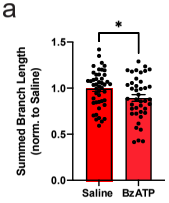

Supplementary Figure 3.

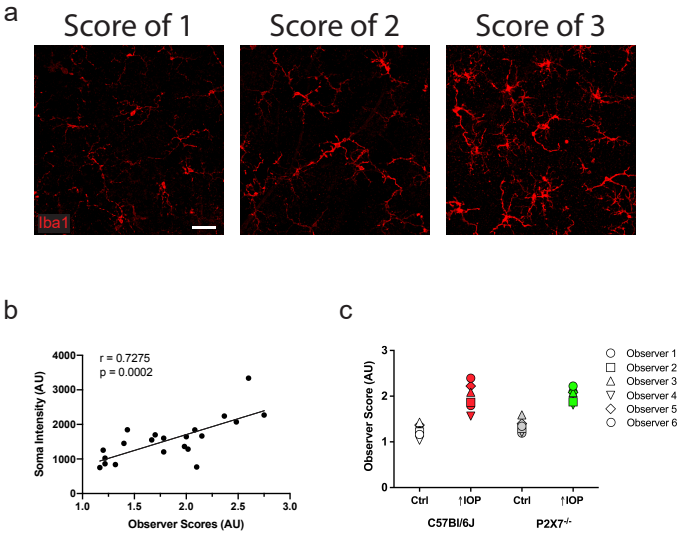

Supplementary Figure 5.

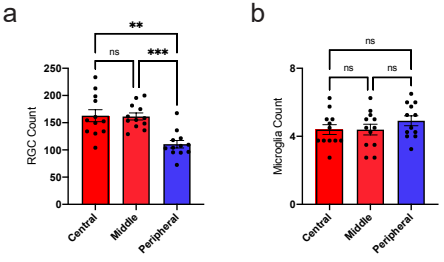

Figures

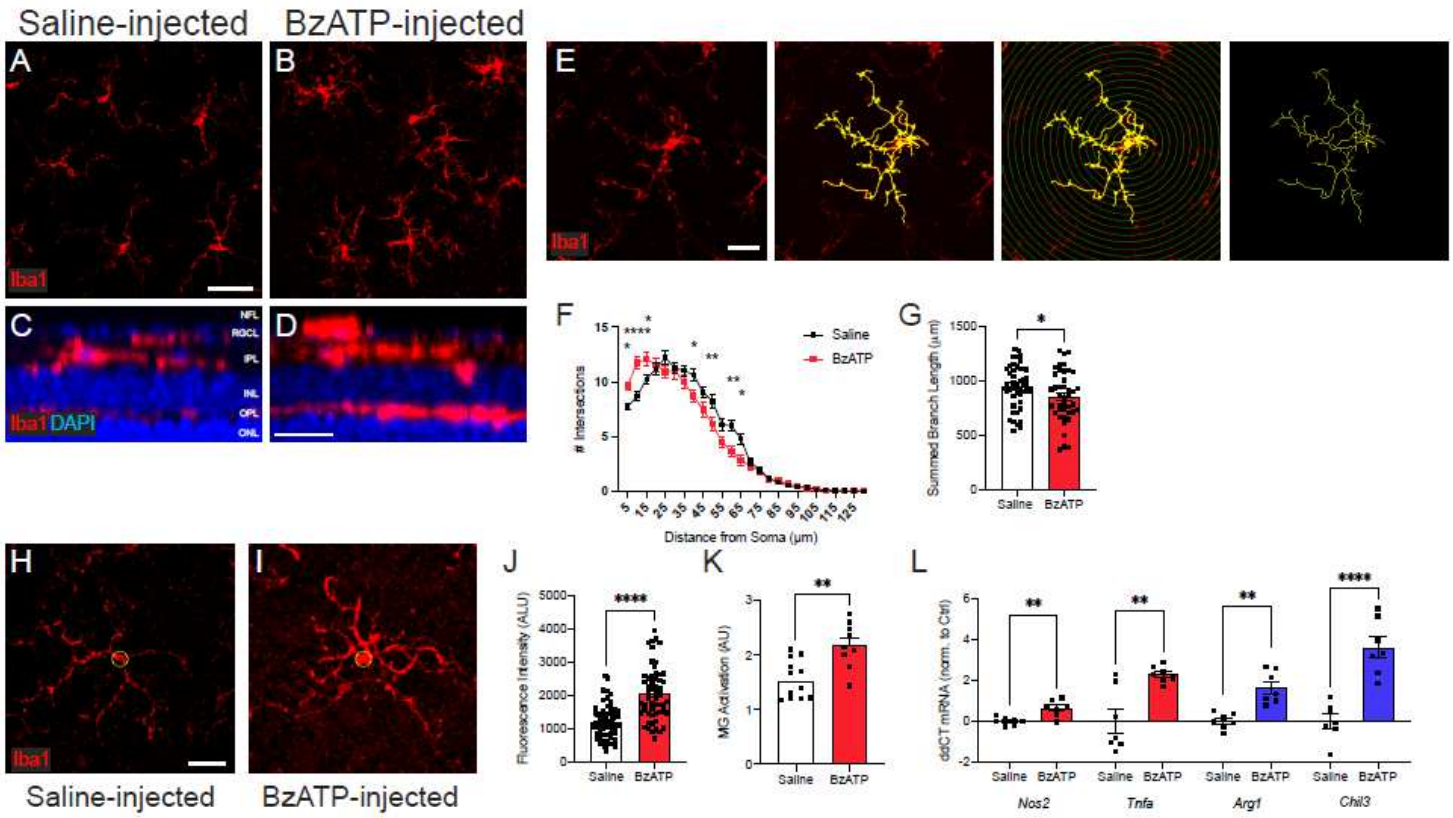

Figure 1

Retinal P2X7R stimulation leads to activated microglia morphology and gene expression. a, b Retinae injected with Saline or 250 µM BzATP indicated that BzATP exposure results in greater Iba1 expression and different morphology. c, d Z-projections of retina wholemounts demonstrate increased Iba1 staining in the IPL and RGC layers of the retina with BzATP exposure. e. Representations of image tracing and conversion to a binary image for analysis. f. Sholl analysis indicates reduced branching complexity of microglia exposed to BzATP (n = 41, 46 cells, 3 biological replicates). g Summed branch length is reduced in microglia exposed to BzATP. When compared to Saline (h), Cell soma size and Iba1 Intensity are elevated in circled area of microglia from retinae exposed to BzATP (i). j Quantification of Iba1 intensity in selected area (n=60, 55 cells, 3 biological replicates). k Observer scoring of images taken from Saline exposed or BzATP-exposed retinae supports data indicating that Iba1-positive microglia are activated upon exposure to BzATP. Each dot represents the mean value of 6 trained observers (n = 12, 9 images, 3 biological replicates). l Expression of classical activation genes Nos2, Tnfa, and alternative activation genes Arg1, Chil3 is elevated in retinae exposed to BzATP. Statistical significance shown at *p<0.05, **p<0.01, ****p<0.0001. Scale bars represent 40 µm (a), 15 µm (d), 25 µm (e, f).

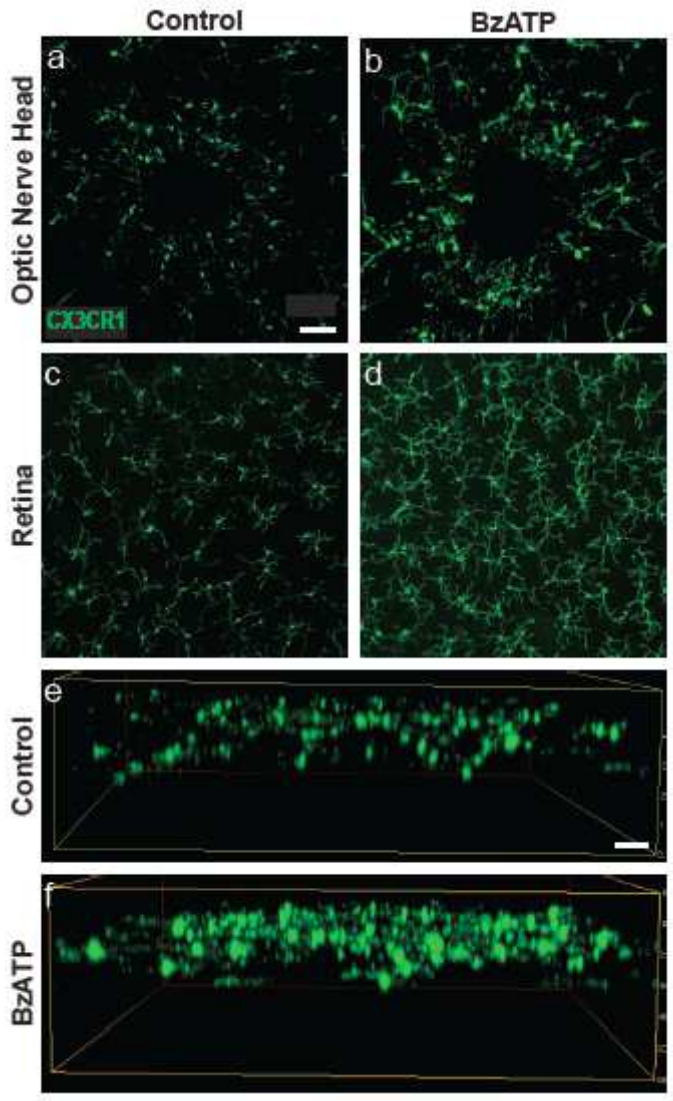

Figure 2

Ex vivo retinal wholemount P2X7R stimulation activates microglia. Retinal whole mounts isolated from Cx3CR1-GFP mice revealed increased fluorescence at the optic nerve head compared to control media (a) after exposure to 200 μM BzATP for 2 hours (b). This elevation in fluorescence was also seen in the Middle Nasal areas when compared to control media (c) or after exposure to BzATP (c). d, e Z-projection of Middle-Nasal retinae exposed to control media or BzATP. Scale bar represents 50 μm.

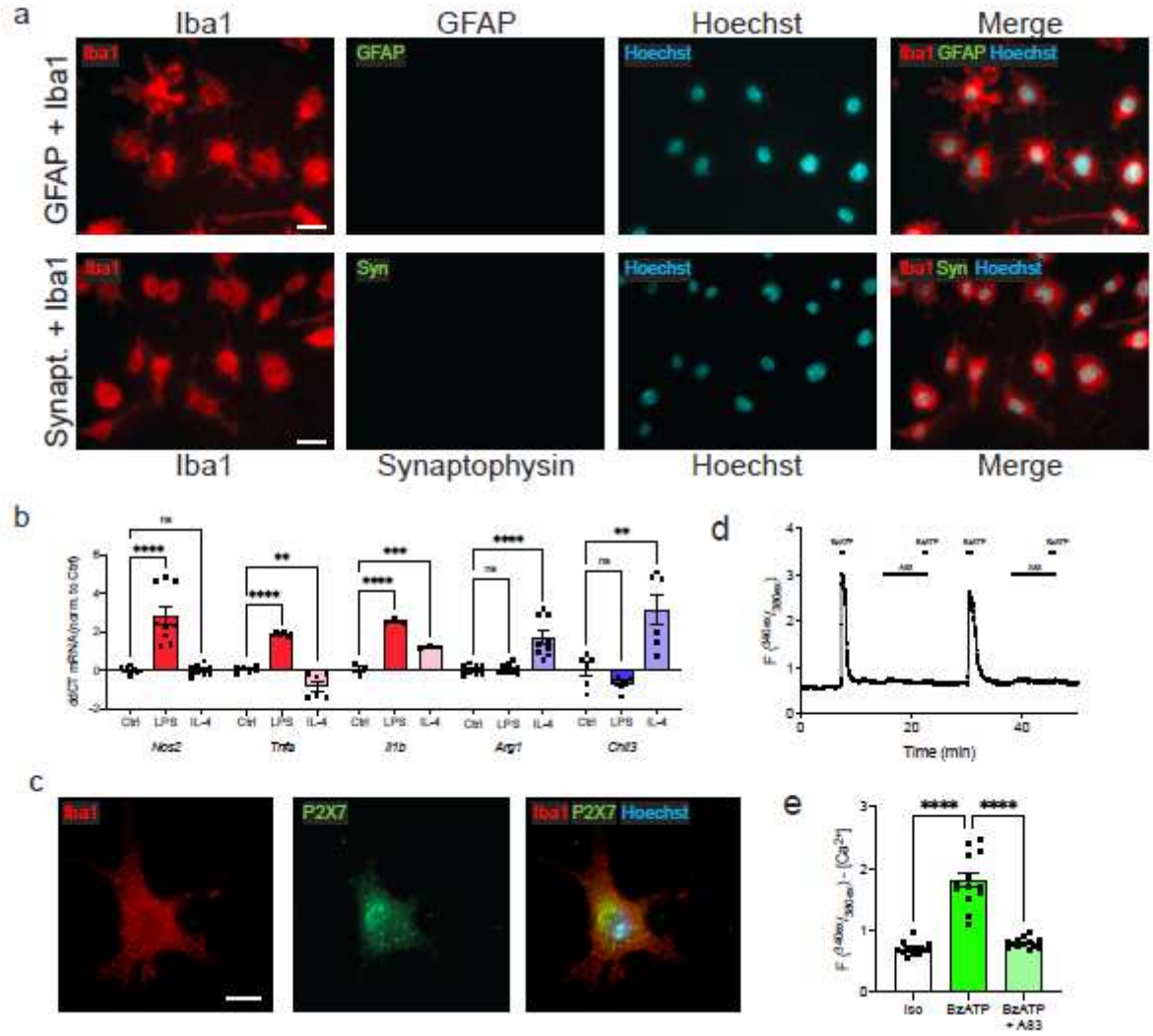

Figure 3

Isolated microglia express functional P2X7 receptor. a Immunocytochemistry indicating absence of GFAP or synaptohysin in primary cultures of retinal microglial cells. b qPCR results from cultured retinal microglial cells exposed for 4 hrs to DMSO (Ctrl), 10 ng/ml LPS (LPS), or 10 ng/ml IL-4 (IL4), with changes in relative expression of mRNA for Nos2, Tnfa, Il1b, Arg1, and YM1 were consistent with microglial cells polarization. (n=6-9 samples from 2-3 biological replicates). c Immunostaining indicated presence of P2X7 receptor in primary retinal microglial cells. d Representative trace from a retinal microglia cell loaded with Fura-2 showing an elevation in the cytoplasmic Ca2+ levels in response to 1 min BzATP (100 μM). The signal is displayed as the ratio of light excited at 340/380 nm and emitted > 520 nm. The response to BzATP was reduced with exposure to 1μM antagonist A839977 (A83) but restored upon wash out. e Quantification of the increase in the ratio of light excited at 340nm vs. 380nm, em >520 nm (referred to as “F 340/380”), indicative of cytoplasmic calcium in cells loaded with Fura-2 (n=3-6 cells/replicate, 3 biological replicates. Statistical significance shown at **p<0.01, ***p<0.001, ****p<0.0001. Scale bar represents 20 μm (a), and 10 μm (c).

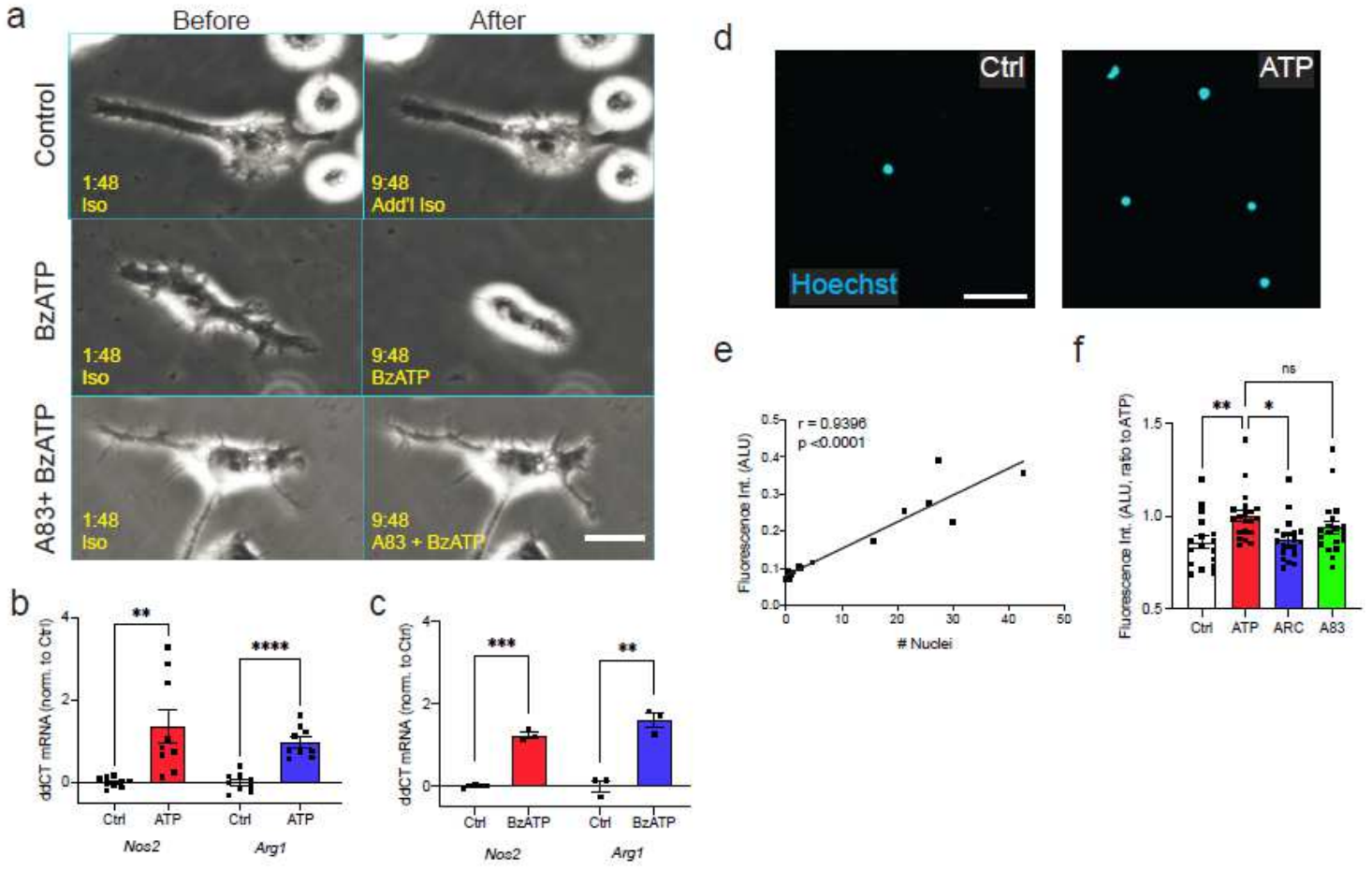

Figure 4

Isolated retinal microglia respond to P2X7 receptor stimulation with activation and retraction a Images taken before and after application of isotonic solution (Control), 250 μM BzATP or 250 μM BzATP + 10 μM A839977 (A83). In cells preincubated with 10 μM A839977, BzATP did not alter cell size much. Similar responses were found in >7 experiments. b Elevated expression of classical activation marker Nos2 and alternative activation marker Arg1 in cultured retinal microglial cells exposed to 1 mM ATP for 4 hrs (n=9-10 samples, 3 biological replicates). c Similar gene expression changes were observed when microglial cells were exposed to 200 μM BzATP for 4 hrs (n=3 tests, 1 biological replicate). d Representative images of migration 2-part Boyden chamber kit filter indicated that microglia migrate towards a 1 mM ATP gradient. e Microglia were isolated from murine brain and subjected to migration. Correlation between number of Hoechst-stained nuclei per well and fluorescence at 340ex/527em (Pearson's correlation r=0.9396 with p=0.0001). f Microglia migration to 1 mM ATP was inhibited with preexposure to 10 μM P2Y12 inhibitor AR-C 69931 (ARC) but not 1 μM P2X7-inhibitor A83 (n=17-20 samples, 4 biological replicates). Statistical significance shown as *p<0.05, **p<0.01, ***p<0.001, ****p<0.0001. Scale bars represent 10 μm (a), 50 μm (d).

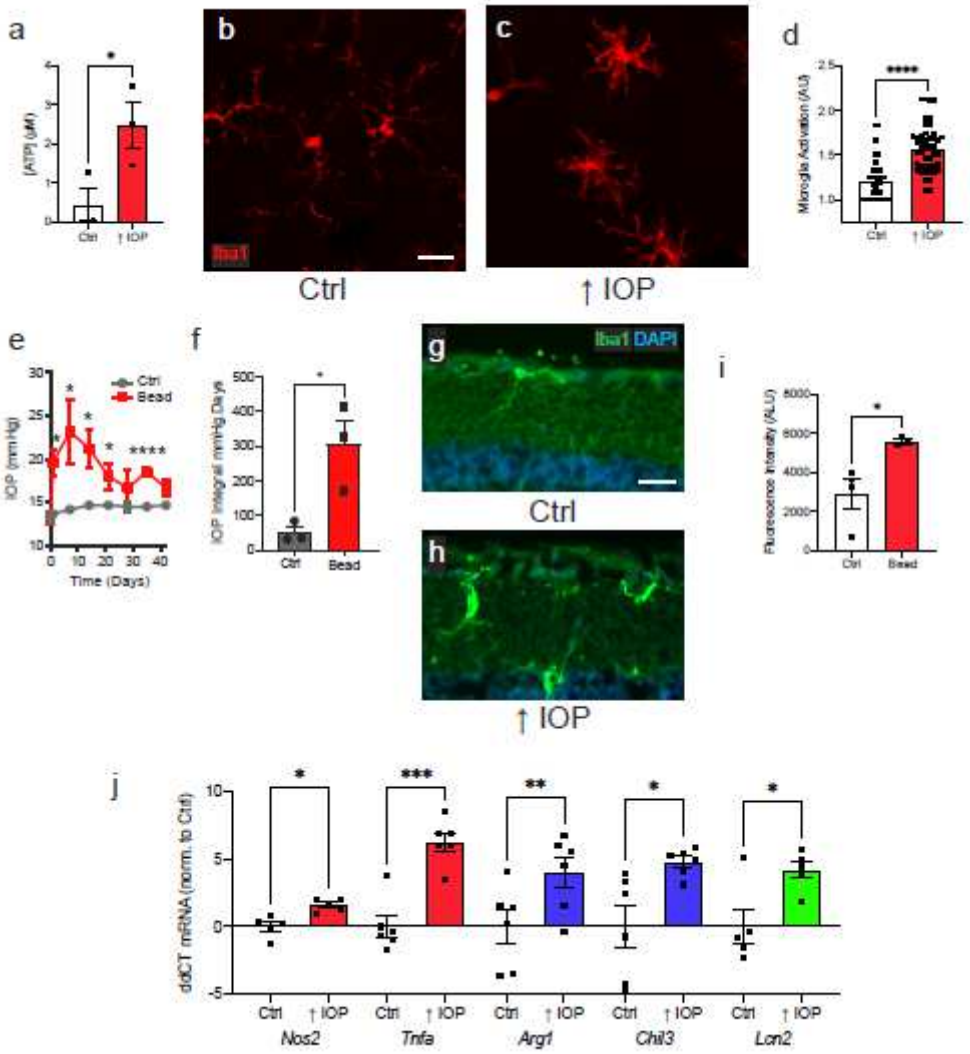

Figure 5

Elevation of IOP releases ATP and activates microglia. a Increase in ATP concentration of vitreous humor 24 hrs after elevation of IOP via the controlled elevation of IOP (CEI) procedure (n=3 biological replicates). b Immunohistochemical image showing staining for Iba1 (red) in the central nasal quadrant in a retinal whole mount from an unstimulated C57Bl/6J mouse eye. c Iba1 staining from an analogous region of an eye after elevation of IOP, and sacrificed 24hrs later. Retinal microglia subject to IOP elevation showed increased soma s 845 ize, increased staining for Iba1, and shorter, thicker projections. d Quantification of morphological activation of microglia across central and middle regions (n=48, 47 images, 3 biological replicates). e Weekly IOP measurements from mice injected with magnetic beads or saline control (n=3). f IOP integral, expressed as summed mmHg days exposure over baseline IOP, for bead and saline-injected eyes. g Immunohistochemical staining of Iba1 of a cryosection of the central region of saline injected eye outlines elongated processes. h Iba1 staining of an analogous region of a retina subjected to 7 weeks of elevation of IOP indicates microglial phenotype emblematic of activation. i Quantification of a 5 µm area surrounding the soma indicates significant elevation of Iba1 intensity per cell (n=4 retinae, 3 mice). j qPCR showing increased expression of Nos2, Tnfa, Arg1, and Chil3, as was Lcn2 in the retina 24 hrs after

the CEI procedure. Dots represent change in expression from a single mouse, with expression normalized to the average of unpressurized contralateral eyes (n=4-7 mice). Scale bars represent 20 μm (b) and 50 μm (g). Statistical significance shown as *p<0.05, **p<0.01, ****p<0.0001.

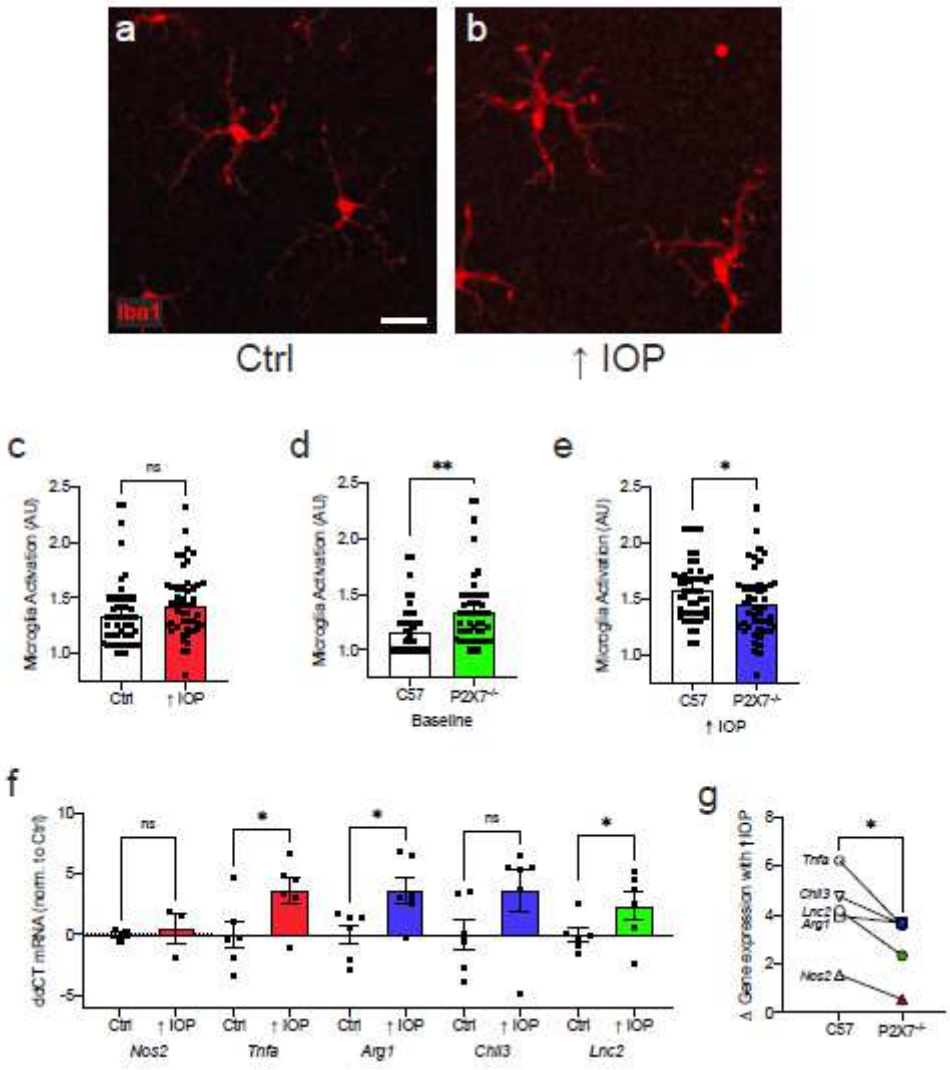

Figure 6

P2X7 receptor is implicated in microglia activation in vivo. a Iba1 staining central nasal quadrant retinal whole mount of P2X7-/- mouse under baseline conditions. b Immunohistochemical staining of an analogous region 24 hrs after IOP elevation in P2X7-/- mice. c Observer scoring of IHC images of microglial morphology across central and middle regions of P2X7-/- mice suggests no differences between baseline (clear) and CEI (red) (n=48 images, 3 mice). d Scoring of baseline conditions was greater in retina from P2X7-/- mice (green) than C57Bl6J mice (clear) (n=48 images, 3 mice). e 24 hrs after elevation of IOP, microglial activation scores were greater in C57 mice than P2X7-/- mice (3 Ctrl, 3 P2X7-/- mice). f Increase in retinal expression of Arg1, TNFa, iNOS, Chil3 and Lcn2 found 24 hrs after the CEI procedure in P2RX7-/- mice (n=3-6 mice). g Relative change in retinal expression of key genes after the CEI procedure in C57Bl/6J mice compared to P2RX7-/- mice. Values represent mean ΔΔCT levels for

each gene compared to unpressurized control retinae. Scale bar represents 20 µm. Statistical significance shown as *p<0.05, **p<0.01.

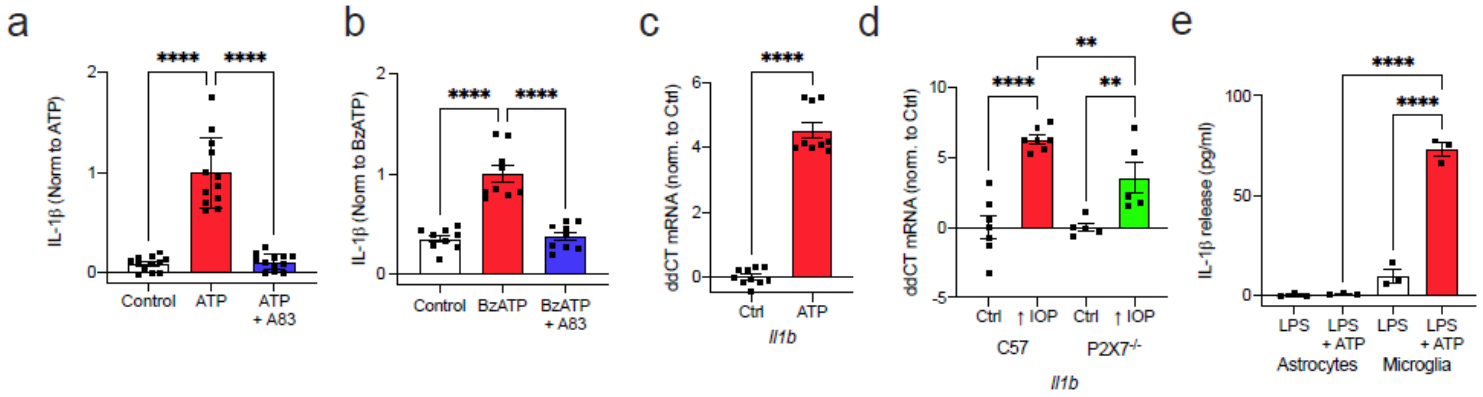

Figure 7

P2X7 receptor stimulation releases cytokine IL-1β. a Mouse retinal microglial cells primed with 1 µg/ml LPS for three hours then exposed to an additional 3 mM ATP released a significant quantity of IL-1β protein into the supernatant relative to LPS alone (Control). Preincubation with 1 µM A83 abolished release (n=12 samples, 4 biological replicates). b Similar pattern of IL-1β release was measured in primed microglial cells with 1 hr exposure to 200 µM BzATP (n=9 samples, 3 biological replicates). c Gene expression of Il1b was elevated in cultured mouse retinal microglia after 4 hr exposure to 1 mM ATP. d Gene expression of Il1b was upregulated in C57B67 and P2X7-/- retinae after elevated IOP, but that upregulation was significantly less in P2X7R-/- retinae (n=6, 5 mice). e Rat microglia primed with 500 ng/ml LPS for 3 hours followed by exposure to an additional 3 mM ATP released significantly more IL-1β than cultured rat astrocytes primed with LPS and 5 ng/ml IL-1α, followed by similar exposure to ATP (n=3 samples from cultures obtained from multiple rats combined). Statistical significance shown as *p<0.05, ****p<0.0001.

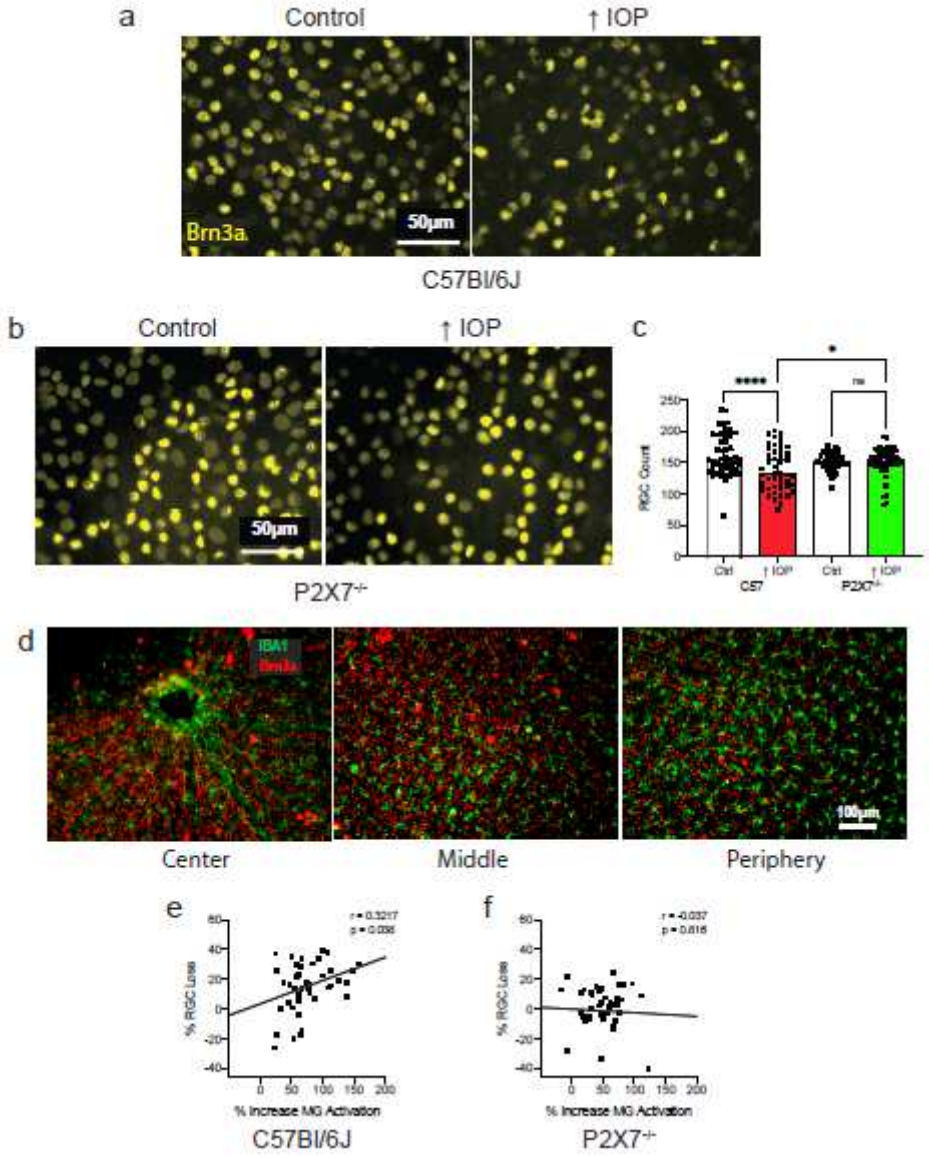

Figure 8

Ganglion cell death is correlated to P2X7R stimulation and 888 microglial activation. a Representative images show that staining for RGC marker Brn3a is decreased in retina 22 – 24 hrs after IOP elevation following IOP elevation to control C57Bl/6J mice. b Decrease in Brn3a staining was not observed in retinae from P2X7-\- after IOP elevation compared to control. c Fewer Brn3a-labeled RGCs were counted in retinae from C57Bl/6J eyes exposed to elevated IOP (red) compared to normotensive controls (clear, left). RGC numbers in control (clear, right) and elevated IOP (green) in P2X7-/- mice were unchanged, demonstrating that there is no pressure dependent loss of RGCs in the P2X7-/- mice. More Brn3a cells were quantified from P2X7-/- eyes subjected to elevated IOP (green) compared to C57 eyes (red) (n= 42-46 images, 3 mice). d Retinal whole mount from a C57Bl/6J mouse showing the spatial relationship between RGCs stained with Brn3a (red) and Iba1 stained microglial (green); images show staining across the central region with the optic nerve head (left) the middle region (center) and peripheral region (right) of the optic disk are shown. e Correlation between the loss of RGCs and rise in microglial activation

accompanying IOP elevation. (Pearson’s correlation with p=0.038; n=7 sections from central and middle regions of 3 control and contralateral CEI retina). f No such correlation between RGC loss and microglial activation exists in regions from P2X7-\- mice. Statistical significance show as *p<0.05, ****p<0.0001.

Supplementary Files

This is a list of supplementary files associated with this preprint. Click to download.

- ExtractPage.pdf
- FigS4aControlIsojpegcompressed.avi
- FigS4bBzATPjpegcompressed.avi
- FigS4cA83Bzjpegcompressed.avi